BASIC PRINCIPLES OF UNCONVENTIONAL GYROS

by

DEREK HOWARD BAKER, LT., RCN
B.S. in E.E., University of New Brunswick, 1957

JAMES WEATHERSPOON HARRILL, CAPT., USAF
B.S. in E.E., North Carolina State College, 1958

SUBMITTED IN PARTIAL FULFILLMENT
OF THE REQUIREMENTS FOR THE
DEGREE OF MASTER OF SCIENCE

at the

MASSACHUSETTS INSTITUTE OF TECHNOLOGY
May, 1964

Signature of Authors_____

Department of Aeronautics
and Astronautics, May 1964

Certified by_____
Thesis Supervisor

Accepted by_____
Chairman, Departmental
Graduate Committee

BASIC PRINCIPLES
OF
UNCONVENTIONAL GYROS

by

Derek H. Baker
James W. Harrill

Submitted to the Department of Aeronautics and Astronautics on May 22, 1964, in partial fulfillment of the requirements for the degree of Master of Science.

ABSTRACT

The basic principles of four representative unconventional gyros are developed. The force between the plates of a charged capacitor manifests itself as the basis for rotor support in the electrostatic gyro. The cryogenic gyro support is dependent on the unusual electric and magnetic behavior of metals at extremely low temperatures. The laser gyro utilizes high frequency electromagnetic radiation instead of angular momentum to sense inertial rotations. The angular momentum of the nuclear gyro is that of sub-atomic particles of matter.

Thesis Supervisor: Robert K Mueller
Title: Associate Professor of Aeronautics and Astronautics

ACKNOWLEDGEMENTS

The authors wish to express their appreciation to Dr. R. K. Mueller who served as thesis supervisor, to Mr. A. J. Smith of the Inertial Gyro Group who assisted in the preparation and organization, and to all the personnel of the Instrumentation Laboratory, Massachusetts Institute of Technology, who directly or indirectly assisted in the preparation of this thesis.

The publication of this thesis was made possible through the support of DSR Project 52-192, sponsored by the Navigation and Guidance Laboratory of the Aeronautical Systems Division AFSC through Contract AF 33(~~616~~)-~~7281~~ 657-7668.

The publication of this report does not constitute approval by the Air Force of the findings or the conclusions contained therein. It is published only for the exchange and stimulation of ideas.

TABLE OF CONTENTS

CHAPTER 1

INTRODUCTION

A conventional gyro is here defined to be one where the angular momentum is developed by a spinning wheel of macroscopic dimensions supported by physical contact with its surrondings. Although developed to a high standard of performance, gyros of this type do have inherent limitations. As a result, a number of unconventional gyros are under development.

The open literature contains numerous reports on the development of unconventional gyros. All too often, however, these reports contain only the results of a particular development and not the basic principles upon which they are based. The present authors are of the opinion that this lack of scaffolding severely limits widespread comprehension. It is in the interest of the fullest utilization of knowledge that this report was undertaken.

As a first cut at this task, the authors have chosen four unconventional gyros to describe. Available time did not allow the inclusion of others. The four

chosen are the electrostatic, the cryogenic, the laser, and the nuclear. They will be discussed in that order in separate chapters. Each chapter is intended to stand by itself, and any one may be read separately.

The electrostatic gyro will be the first of these four to become operational. It is unconventional in the sense that the spinning mass is supported without contact by an electric field. The cryogenic is the magnetic analogy of the electrostatic gyro. The laser device is truly unconventional by any gyro man's standards; there is no angular momentum. The nuclear gyro represents a radical departure from conventional thoughts; the angular momentum is that of sub-atomic particles of matter.

Although each of these gyros has some advantage over the others and over conventional instruments, it is not our purpose to sell one over any other. Instead, the basic principles of each will be presented in such manner as to appeal to the reader's intuition and to complement his background in conventional gyros.

As students in the Department of Aeronautics and Astronautics at MIT, the authors often wished for a report of this nature but found none available. In order for this report to be available to all who seek it, all material is from non-classified sources. Furthermore, we recommend that other reports be undertaken to similarly cover other unconventional gyros.

Insofar as is practical, notation is consistent from chapter to chapter and is in accordance with the various established disciplines of science. References are indicated in the text by number and set apart by parentheses, for example (28). References will be found at the end of the report grouped by chapters.

CHAPTER 2

ELECTROSTATIC GYRO

2.1 Introduction

The spinning mass which yields the angular momentum of convential gyros is supported by ball bearings which although good, result in long term drift. This drift can be eliminated if some means of support without contact, i.e. field support, can be found. The spinning mass of the electrostatic gyro is so supported without contact.

Professor Arnold Nordsieck of the University of Illinois was among those investigating field support in the early 1950's. Magnetic fields are able to provide the necessary support; but because of eddy current losses, hysteresis losses, and rotor magnetic moment, undesired torques result (1). In 1952, he invented the Electric Vacuum Gyro now more commonly known as the Electrostatic Gyro (ESG).

Basically the ESG consists of a spinning sphere supported by an electric field. It will be shown that

the sphere and its support system behave as two capacitors in series. To fully understand the support system, an equation for the force between the plates of a capacitor will be developed from basic principles. It will be shown that without compensation this type of suspension is unstable. The characteristics of an RLC (Resistance, Inductance and Capacitance) circuit provide a simple means of stabalizition and pertinent equations will be developed. Angular velocity of the sphere is provided by induction motor techniques. A simplified approach to induction motor theory will be presented. A general discussion of the characteristics of a typical ESG will follow the presentation of basic theory.

2.2 Capacitance of a Parallel Plate Capacitor (2,3)

A development of the equation of force between plates of a capacitor logically begins with a discussion of capacitance.

The most common and perhaps best known definition of capacitance is

$$C = \frac{q}{V} \qquad (2.1)$$

where C is the capacitance measured in farads; q, the charge on one plate measured in coulombs; and V, the potential difference between the plates measured in volts.

Although Equation (2.1) does give a formula for capacitance it will be seen that a formula for capacitance that is a function of the physical dimensions of the capacitor will be necessary in our derivation.

To understand the derivation of capacitance that will follow it is first necessary to develop alternate expressions for both q and V in Equation (2.1). This requires an understanding of electrostatics.

The starting point for any study in electrostatics is Coulomb's Law which states that the force between two charged bodies is proportional to the product of the magnitude of the charges divided by the square of the distance between them. This is an experimental law and is written as follows

$$F = \frac{K\, q'q''}{r^2} \qquad (2.2)$$

where q' and q" are the charges on the two bodies in question measured in coulombs; r is the distance between the bodies measured in meters; and K, the constant of proportionality, is determined by the system of units chosen and has the dimensions of newton meters^2/ coulombs^2 in the RMKS system.

The next logical step is a definition of Electric Field Intensity. An electric field exists in a region where an electric charge experiences a force of electrical origin. The magnitude E of electric field in-

tensity at a point is defined as the force on a charge at that point divided by the magnitude of the charge. The direction of the electric field intensity vector is determined by the direction of the force if the charge were positive. In equation form

$$\overline{E} = \frac{\overline{F}}{q} \tag{2.3}$$

One way of viewing electric fields is by drawing imaginary lines of force from positive charge sources to negative charge sources. The direction of the lines of force at a particular point is the direction of the electric field intensity vector $\overline{E}$ at that point. The number of lines of force through a unit area perpendicular to $\overline{E}$ at that point is equal to the magnitude of $\overline{E}$.

Electric field intensity $\overline{E}$ is related to charge q by Gauss' Theorem. This theorem states that if an imaginary closed surface of any shape is constructed in an electric field, the net number of electric lines of force which cut across the surface in an outward direction is equal to $1/e_o$ times the net positive charge which is enclosed by the surface regardless of the way in which the charge is distributed inside the Gaussian Surface. That is

$$\int_A E_n dA = \frac{1}{e_o} q \tag{2.4}$$

where e_o is the permittivity of free space and has the

value 8.85×10^{-12} coulombs^2/ newton meters^2. E_n is the normal component of electric field intensity at the surface. The integration is carried out over the entire area A of the Gaussian surface.

With this theorem we are now in a position to determine the Electric Field Intensity between the plates of a charged parallel plate capacitor. See Figure 2-1a. Let us consider a rectangular Gaussian surface CDFG and unit length into the paper. Assume also that the charge on the plate of the capacitor has surface density σ coul/m^2. It is seen from the figure that the only area out of which electric lines of force are emanating is side DF. Therefore

$$\int_{DF} E_n dA = E \int_{DF} dA = \frac{1}{e_o} A' \qquad (2.5)$$

where A' is the area CG. Therefore, after integration the electric field intensity is

$$E = \frac{1}{e_o} \sigma \qquad (2.6)$$

If fringing at the edges of the plates is neglected (this assumption is valid if the distance between the plates is small compared with any linear dimension of the plates) Equation (2.6) gives the electric field intensity at any point between the two parallel plates.

Potential Difference or V between two points is defined as the change in potential energy of a test

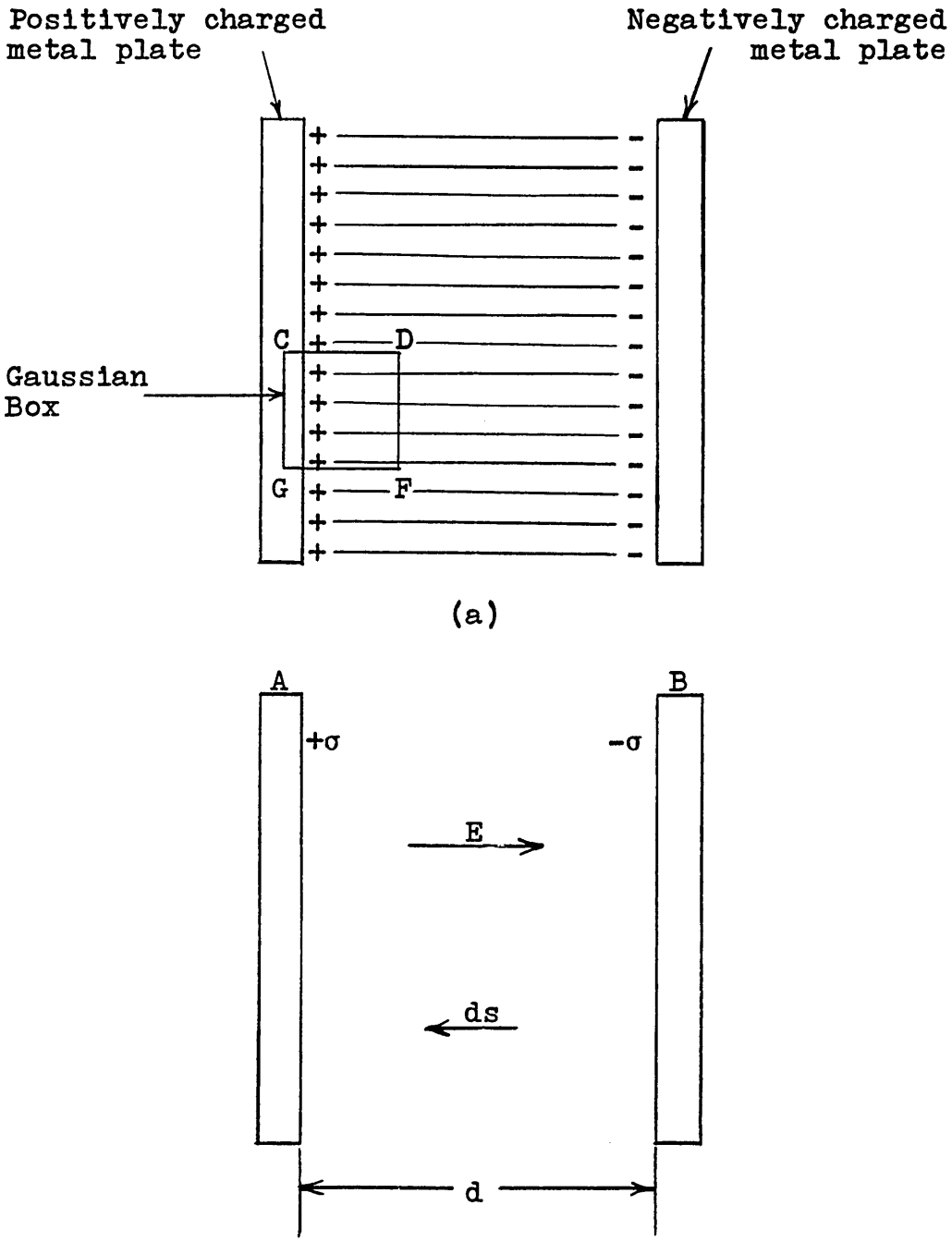

FIGURE 2-1

ELECTRIC FIELD BETWEEN PLATES OF A CAPACITOR

charge when it is moved between the two points divided by the magnitude and sign of the test charge. Change in potential energy is the negative of the line integral of the dot product of a force and the distance over which it acts. In differential form

$$d(PE) = -\overline{F}.\overline{ds} \tag{2.7}$$

Equation (2.3) gives the electrostatic definition of $\overline{F}$. Referring to Figure 2-1b and our definition of potential differance given above we see that the potential difference in volts between the plates is

$$V_A - V_B = \int_d \overline{E}.\overline{ds} \tag{2.8}$$

Noting that $\overline{E}$ is constant between the plates and parallel to $\overline{ds}$; integration yields

$$V_A - V_B = Ed \tag{2.9}$$

where d is the distance between the plates. Substituting Equations (2.9) and (2.6) into Equation (2.1) and noting that σ is q/A gives a value for C which is

$$C = \frac{A}{d}e_o \tag{2.10}$$

where A is the area of either plate and d the distance between them. If we desire the capacity in a medium other than free space the formula will be

$$C = \frac{KA}{d}e_o \tag{2.11}$$

where K is the relative dielectric constant and is

dimensionless. K is 1 for free space and greater then 1 for other media. As we will see, however, Equation (2.10) will be the more appropriate one because the medium with which we will be concerned will be a vacuum (i.e. free space). Equation (2.10) is thus our alternative expression for capacitance in terms of physical dimensions.

2.3 Force Between Plates of a Capacitor (3)

It is now required to determine the force between the two plates of a capacitor.

Referring to Figure 2-2 we wish to determine the force on a unit positive charge q at point O due to all the charges on the negatively charged upper plate. Considering the elemental area on the plate as a ring and referring to Equation (2.2) it is seen that the force on the charge at O due to charges on the ring will be directed along R. The components of the force parallel to the plate when summed around the ring will net to zero and only the components normal to the surface will affect q. Therefore, the elemental force at O due to charges on the ring is

$$df = \frac{K(2\pi r\sigma dr)q}{R^2}\cos\phi \qquad (2.12)$$

where σ is surface charge density on the ring. Let $d\omega$ represent the element of solid angle which the area of the ring subtends at O; therefore,

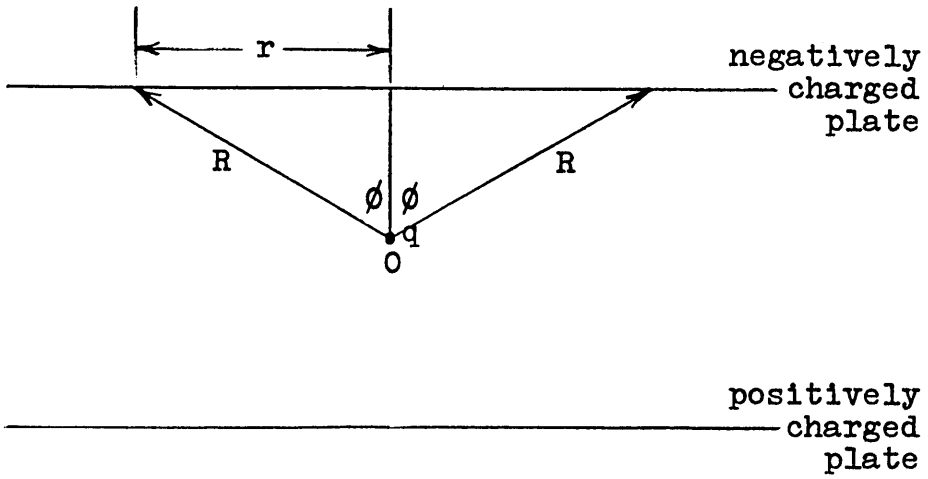

(a)

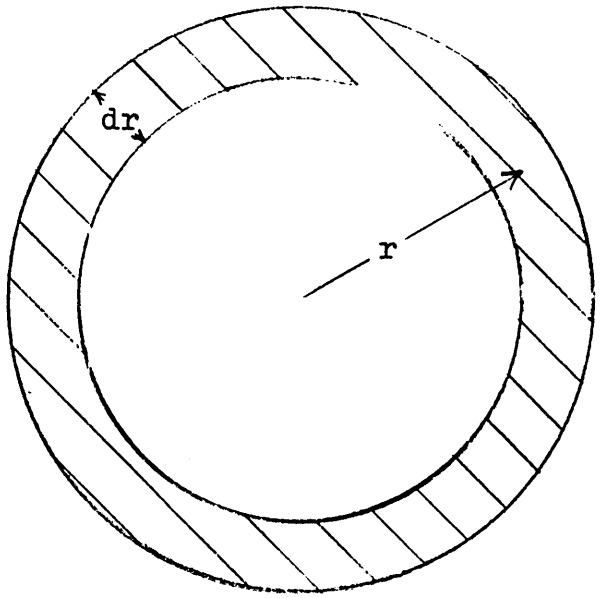

(b)

FIGURE 2-2

FORCE BETWEEN PLATES OF A CAPACITOR

$$d\omega = \frac{2\pi r dr}{R^2}\cos\phi \qquad (2.13)$$

Substituting in Equation (2.12) gives

$$df = K\sigma q d\omega \qquad (2.14)$$

Integrating over the whole solid angle and noting that the whole angle is 2π we get

$$f = K\sigma q 2\pi \qquad (2.15)$$

In RMKS units

$$K = \frac{1}{4\pi e_o} \qquad (2.16)$$

Substituting in Equation (2.15) gives

$$f = \frac{\sigma q}{2e_o} \qquad (2.17)$$

where f is a force of attraction. Note that this force is independant of q's distance from the plate.

Let us now consider the force exerted by the upper plate on an elemental charge dq on the lower plate. The elemental force will be

$$df = \frac{\sigma dq}{2e_o} \qquad (2.18)$$

If this equation is integrated over all the elemental charges on the lower plate, we see that Equation (2.17) results where q is now the total charge on the lower plate. The charge on the upper plate is equal in magnitude to the charge on the lower plate and therefore

$$\sigma = \frac{q}{A} \qquad (2.19)$$

where A is the area of one of the plates. Substituting in Equation (2.17) we see that the total force exerted by one plate on the other is

$$F = \frac{q^2}{2e_o A} \tag{2.20}$$

Substituting Equations (2.1) and (2.10) into Equation (2.20) gives the result

$$F = \frac{Ae_o}{2}\left(\frac{V}{d}\right)^2 \tag{2.21}$$

which is the force of attraction between the plates of a capacitor in terms of the voltage difference between the plates and the distance between them. Thus we have the phenomena of force without contact. If this phenomena is to be exploited in a system of suspension where contact is not allowed, then a curve of force of attraction vs separation distance must have positive slope. Observe in Equation (2.21) that at constant V, a decrease in separation distance results in an increased force of attraction; i.e., the slope of the F vs d curve is negative. Hence, some means must be found to vary V as a function of d such that the F vs d curve has positive slope. The next section develops a technique whereby this is accomplished.

2.4 Series RLC Circuit

Let us consider an RLC series circuit to which is applied an AC voltage V_i Sin ωt. See Figure 2-3a. The current i through the circuit is

$$i = \frac{V_i}{R+(X_L+X_C)} \tag{2.22}$$

where

$$X_L = j\omega L \tag{2.23}$$

$$X_C = 1/j\omega C \tag{2.24}$$

The voltage V_C across C is

$$V_C = iX_C$$

$$V_C = \frac{V_i X_C}{R+(X_L+X_C)}$$

Substituting Equations (2.23) and (2.24) for X_L and X_C gives

$$V_C = \frac{V_i}{(1-\omega^2 LC)+j\omega RC} \tag{2.25}$$

Let us now substitute the results of Equation (2.10) in Equation (2.25). Also for simplicity let us assume V_i is a unit input. This yields

$$V_C = \frac{1}{(1-\omega^2\frac{LA}{d}e_o)+j\omega\frac{RA}{d}e_o} \tag{2.26}$$

Dividing both sides of the equation by d gives

$$\frac{V_C}{d} = \frac{1}{(d-\omega^2 LAe_o)+j\omega RAe_o} \tag{2.27}$$

$$\left|\frac{V_C}{d}\right| = \frac{1}{\sqrt{(d-\omega^2 LAe_o)^2+(\omega RAe_o)^2}} \tag{2.28}$$

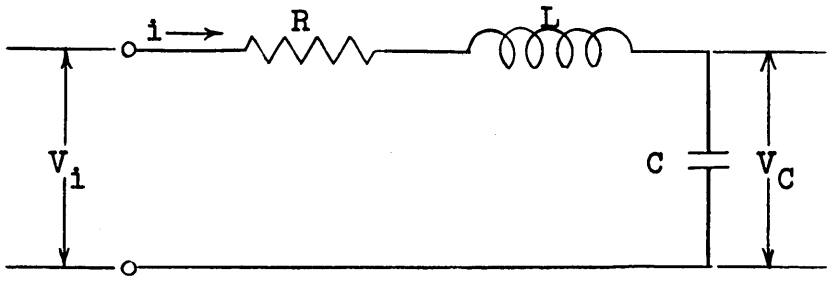

(a)

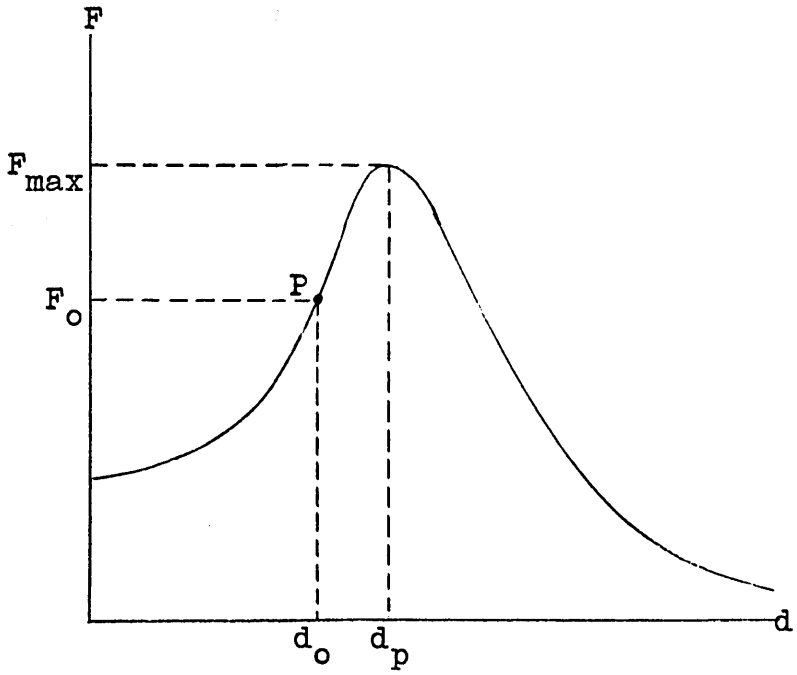

(b)

FIGURE 2-3

SERIES RLC CIRCUIT AND

CAPACITIVE FORCE VS DISPLACEMENT CURVE

squaring

$$\left|\frac{V_C}{d}\right|^2 = \frac{1}{(d-\omega^2 LAe_o)^2+(\omega RAe_o)^2} \qquad (2.29)$$

Multiply both sides of the equation by $Ae_o/2$ and referring to Equation (2.21) gives

$$F = \frac{Ae_o}{2} X \frac{1}{(d-\omega^2 LAe_o)^2+(\omega RAe_o)^2} \qquad (2.30)$$

If this equation is plotted as F vs d (Figure 2-3b) we observe that in the region to the left of the peak the slope is positive. If we can operate in this region of the curve, the condition for stable suspension as outlined in the previous section is satisfied. Note that the peak of the curve occurs at

$$d_p = \omega^2 LAe_o \qquad (2.31)$$

and that the maximum force is

$$F_{max} = \frac{Ae_o}{2} X \frac{1}{(\omega RAe_o)^2}$$

$$F_{max} = \frac{1}{2\ \omega^2 R^2 Ae_o} \qquad (2.32)$$

If a point P is established by a desired equilibrium force and displacement, F_o and d_o, the parameters of Equations (2.31) and (2.32) are varied such that the F vs d curve passes through P with positive slope.(4).

2.5 Induction Motor Theory

As noted in the introduction, the angular velocity of the gyro sphere is provided by induction motor techniques. As will be shown in Section 2.8, the sphere, itself, can be considered to be the rotor of an induction motor. Hence, a simplified discussion of induction motor theory is presented. It is not intended here to cover the entire field relating to induction motor theory. If the reader wishes to obtain more detail, any text on alternating current machinery will suffice (5). Instead, only the pertinant details will be covered as necessary to understand the electrostatic gyro.

Induction motors are AC (alternating current) devices and an AC voltage is represented

$$v(t) = V_o \cos \omega t \tag{2.33}$$

A vector representation of v(t) is often used. If we consider a vector of constant length V_o rotating about an origin of coordinates at an angular velocity ω, v(t) of Equation (2.33) is given at anytime as the horizontal projection of the vector. Figure 2-4a shows two such vectors V_a and V_b, both rotating at the same angular velocity ω, which represent two sinusoidal voltages 90^o apart in time phase. The vectors are shown for $t = \pi/4$.

To illustrate the necessary principles let us look

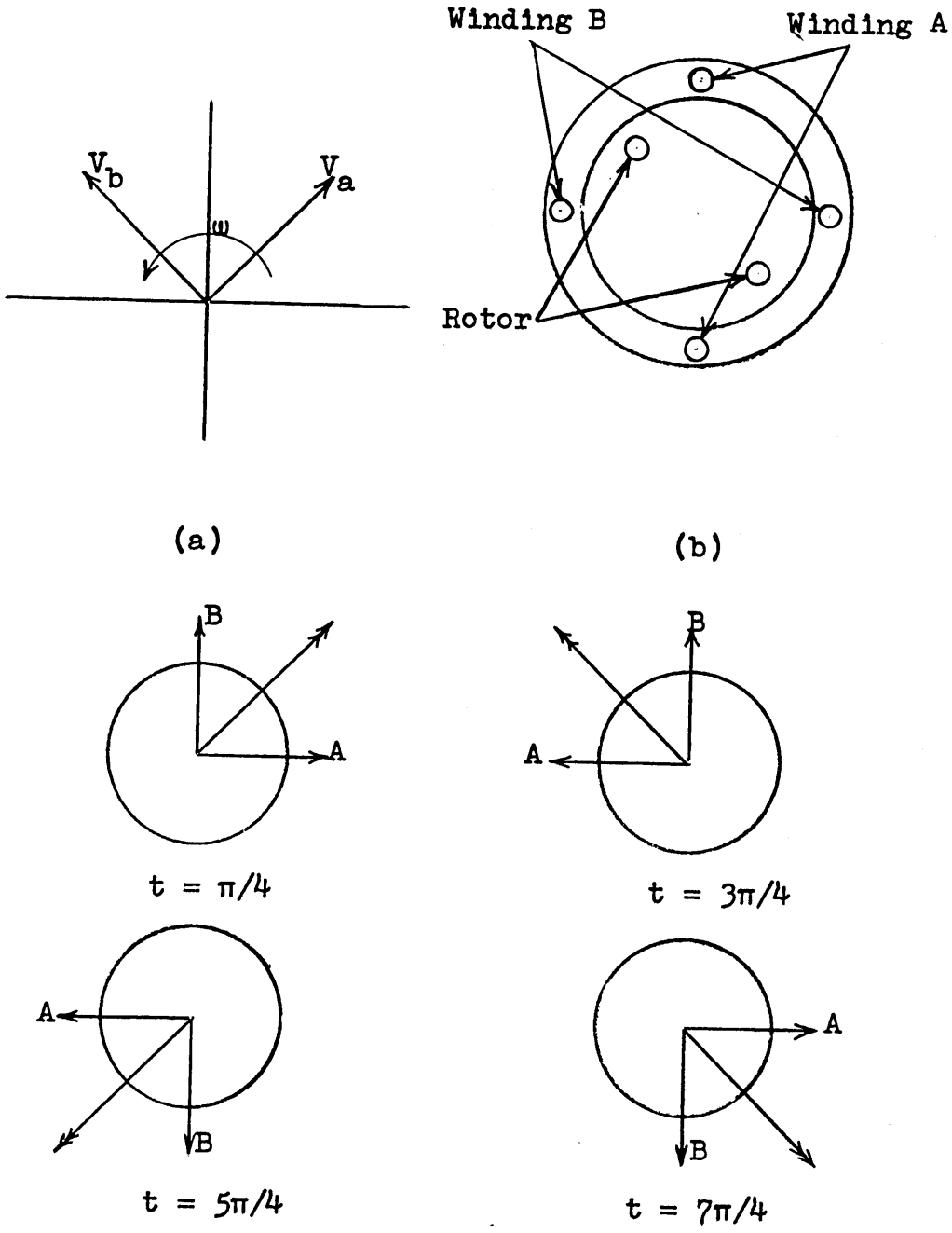

FIGURE 2-4

SIMPLE INDUCTION MOTOR

at a simple two phase induction motor. The motor is made up principally of rotor and stator. Figure 2-4b is a cross-sectional view of the motor. The plane of the paper is normal to the axis of rotation of the rotor. The planes of the windings are also normal to the paper. The two stator windings are normal to each other.

The two voltages represented in Figure 2-4a are fed to the two stator windings. The resulting currents that flow in the windings will produce magnetic fields. As was seen above, the magnitude of the applied voltages varies sinusoidally and therefore, the magnitude of the magnetic fields will also vary sinusoidally. The direction of the magnetic fields will be normal to the two windings.

Let us examine the vector sum of the fields produced by the two stator windings at four different times. See Figure 2-4c. For illustrative purposes we will assume that the fields are in phase with the applied voltages. This in general will not be true; but since the fields bear the same fixed phase relationship with their respective applied voltages, the assumption is valid. Referring to the figure, the time in each case refers to the position of the voltage vectors in Figure 2-4a. In each case the single headed vectors refer to the fields produced by the stator windings A and B; the double headed vector is the vector sum of the two.

We see that the total field produced by the stator is constant in magnitude and rotates at an angular velocity equal to that of the voltage vectors.

The rotor is best illustrated as consisting of a single closed loop. The rotating stator field described above rotates about the rotor winding (assuming for the moment that the rotor is not rotating). Faraday's Law states that a voltage induced in a loop of wire that is cut by magnetic flux is proportional to the rate of change of that magnetic flux. In our particular case the flux is rotating about the rotor loop; therefore, a voltage will be induced in the loop. This loop is a closed one; consequently the induced voltage will cause a current to flow in the loop. This current in turn will produce a magnetic field normal to the plane of the rotor loop. The voltage induced in the loop will be maximum when the stator field vector is aligned with the plane of the rotor loop, and will be zero when it is normal to the plane of the rotor loop. Therefore, the rotor field intensity will vary sinusoidally at a rate equal to the angular velocity of the stator field, but its direction is fixed while the rotor is non-rotating.

In essence, our induction motor consists of two magnets; one of constant magnitude and rotating, the other with a sinusoidally varying magnitude but fixed. Two

magnets whose axes are displaced from each other tend to align with one another. As was seen above one of our magnets is rotating while the other is fixed. It would appear at a glance that the rotor would tend to rotate first in one direction and then the other and that over one period the total rotation would add to zero. However, the rotor field reverses itself twice each period. This causes the net rotation not to be zero. In actual fact the rotor tries to follow the stator field.

The speed at which the rotor finally rotates is slightly less than the speed of the rotating stator field. If the rotor were to rotate at the same speed as the stator field, called "synchronous speed", the rotor loop would no longer be cutting stator flux and in turn would produce no flux itself. Therefore, the rotor will travel at a slightly lower speed, the difference being called "slip frequency".

2.6 Electrostatic Gyro

We are now in a position to look at the ESG in more detail.

Figure 2-5a is a diagram of a representative ESG. It shows the basic elements of such a gyro. A few words about each element would aid in understanding the gyro.

2.7 The Rotor

The rotor, which is the heart of the gyro, attracts

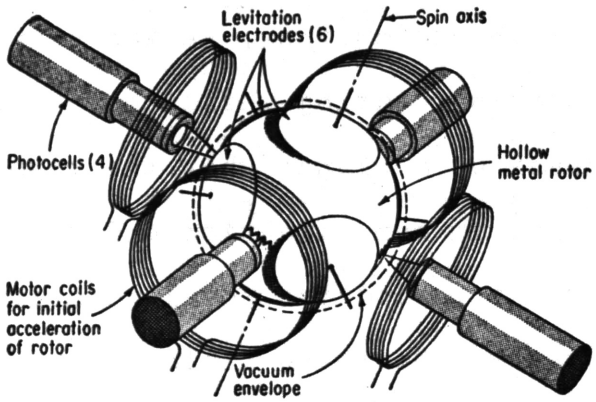

(a)

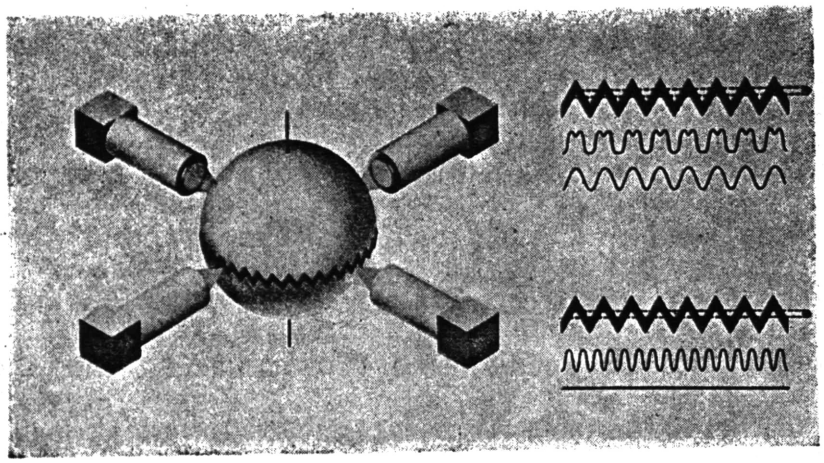

(b)

FIGURE 2-5

ELECTROSTATIC GYRO AND READOUT

(Figure Courtesy of Control Engineering)

our attention first. In order that the rotor be dimensionally stable it is necessary that the rotor material be as stiff as possible. the requirement for dimensional stability is dictated in the design in order that the rotor remain a perfect sphere even when run up to speed. It will be seen in the section on support that unless this requirement is met spurious torques will result. The most logical choice would seem to be a solid rotor. On the other hand, it will be seen that because of limitations in electric field support it is necessary that the rotor be as light as possible. Consequently it is necessary to arrive at a compromise. Materials are chosen that have a high ratio of stiffness to mass. To preclude unnecessary torques due to magnetic fields and at the same time provide a material suitable for electrostatic support, metals that are good conductors but non-magnetic are required. At this particular time Beryllium and Aluminum are used. The rotors are machined hollow with a slight thickening at the equator to provide a preferred axis of rotation. It is made slightly elliptical so that when it is run up to speed it becomes spherical.

2.8 Suspension of the Rotor

Before discussing the field support arrangement it is worthwhile to point out that there are two possible configurations that the ESG can take. The first is the

non-gimballed form. In this system the gyro case is fixed to the vehicle and the rotor axis is free to rotate in any direction with respect to the case. The difficulty with this method is that any torques due to the suspension system vary as the case rotates and it would therefore require a large computor to calculate and provide the necessary corrections.

In the gimballed form the case is kept aligned with the rotor. Any unwanted torques caused by the suspension system can be nulled by a fine adjustment of the electrodes because the torques are constant. The following discussion on the support system will center around this latter type of gyro.

It was seen in Equation (2.21) that a voltage applied to a capacitor generates a force of attraction between the plates. If the rotor is placed between two electrodes (Figure 2-5a) and a voltage is applied to these electrodes, the arrangement resembles two capacitors in series. Thus a force of attraction exists on both sides of the rotor. Three pairs of such electrodes are arranged in orthogonal fashion about the rotor. In order to maximize the force between the rotor and the electrodes, it is necessary to maximize the V/d ratio of Equation (2.21). This ratio, however, is limited by the dielectric strength of the medium. Inasmuch as the dielectric strength of a vacuum is much greater than

that of air, the gyro case is evacuated to pressures of 10^{-7} to 10^{-8} mm of mercury. To support a 25 gram rotor against an acceleration of 4 g's with a gap of 0.010 inches requires a field intensity of 150,000 volts per cm.

The most logical voltage source for support would seem to be DC because an AC voltage with a peak value equal to the DC would have a mean squared value only 1/2 that of the DC. As we have seen, however, DC support is unstable. There are frequent references in the literature to Earnshaw's Theorem in this regard. This theorem states that a charge acted on by electric forces only cannot rest in stable equilibrium in an electric field. Another problem with a DC support field is that should a stray charge exist on the ball it will upset the balance of forces.

It is obvious from the above that even neglecting the possible errors cause by stray charges it is necessary that some sort of feedback be used in a DC system. Knoebel (1) describes a system whereby an AC signal is superimposed on the DC supporting voltage. This AC signal is derived from a high frequency capacitive bridge that measures rotor displacement with capacitive pickoffs situated around the rotor.

A much more desirable and simpler system uses an AC voltage in conjunction with a resistor and an in-

ductor in series with the supporting electrodes. This technique is discussed in Section 2.4. This system, because it is operating in a vacuum, has no damping and must be rate stabilized. Several techniques are discussed in the literature but are considered beyond the intent of this report.

2.9 Bringing Up to Speed

Our next problem is to bring the rotor up to the required operating speed. For this purpose four motor coils are placed in pairs at 90° about the equator of the rotor (Figure 2-5a). If we consider the rotor to be made up of a number of conducting loops in parallel, the system will operate as an induction motor.

A typical operating speed for the rotor is in the range of 10,000 to 30,000 RPM. As was stated previously it is necessary, because of support limitations, to operate the rotor in a vacuum. When the rotor is being run up, heat is generated in it by hysteresis and eddy current losses. The high vacuum limits the rate at which the heat can dissipate to the outer case. This heating of the rotor tends to deform it. It is, therefore, necessary to wait until the heat is dissipated before stable operation can be expected. This takes about a day. In spite of this delay, because the rotor is spinning in a vacuum, there is little drag. Once the rotor is initially accelerated it will coast

for a period of weeks or even months without the requirement of additional acceleration from the motor coils.

If the rotor is initially accelerated with its principal axis not perfectly aligned with the motor spin axis, wobble will result. Two Helmholtz coils (see Sections A5.2 and 5.5) are placed so that the direction of their magnetic field is aligned with the motor spin axis. If the rotor is wobbling, the Helmholtz field will induce currents in the rotor which give rise to torques which bring the rotor principal axis into alignment with the motor spin axis. It should be noted that once the rotor is run up to speed and aligned, neither the Helmholtz nor the motor coils are used.

2.10 Read Out and Alignment of Gyro Case

To determine misalignment of the rotor spin axis with respect to the case, three methods have been proposed. The first utilizes a metallic flange around the equator of the rotor. Pick off electrodes with high frequency bridges provide indication of misalignment. The metallic flange, however, destroys the desired sphericity of the rotor and can cause undesired torques.

Another possible method is to flatten the area at the pole of the rotor and use some type of optical read out. Again the spericity of the rotor is destroyed

and possible undesirable torques can result.

The best method to date utilizes four photomicroscopes. These photomicroscopes are placed in orthogonal pairs about the equator of the rotor (Figure 2-5b). Around the equator of the rotor is a regular saw-tooth pattern. If the rotor is correctly aligned with the case the photomicroscopes will scan the center of the pattern. The resulting sigal from the photomicroscopes will occur at twice the frequency of the zig-zag pattern (see lower right, Figure 2-5b). There will be no signal component that is the fundamental of the zig-zag pattern. If the rotor is out of alignment with the case, we wish to know how far it is out of alignment and in what direction. When the rotor gets out of alignment, the photomicroscopes will scan the pattern either above or below the center line of the pattern. The sketch in the upper right of Figure 2-5b shows the resulting signal when the upper half of the pattern is scanned. We notice that the signal now has the fundamental component present as well as the second harmonic. The magnitude of the fundamental is proportional to the displacement of the scanning line from the center of the pattern. This gives the amount of rotor displacement. Direction of displacement is obtained by comparing the phase of the fundamental with the phase of the second harmonic. As long as the

displacement is less than 1/2 the amplitude of the zig-zag pattern,a second harmonic component will be present with which a phase comparison can be made. The fundamental will be in phase with the second harmonic when the scanning line is above the center line of the pattern and will be out of phase when it is below. Thus we have a means of determining direction and magnitude of rotor displacement. If these signals are fed to the servos which control gyro case position,we are able to keep the case aligned with the rotor spin axis.

In the non-gimballed system the rotor's orientation is arbitrary. To provide read,out coded patterns cover a large portion of the rotor surface;and fixed photo-microscopes view these patterns giving signals which are proportional to the orientation of the rotor spin axis with respect to the case. This system in general is not as accurate as that of the gimballed arrangement.

2.11 Spurious Torques

There are three major causes of spurious torques in the electrostatic gyro. The first is external magnetic fields. If the rotor is spinning in magnetic flux caused by an external magnetic field,currents will be induced in it. As we have seen in Section 2.5 the rotor will attempt to align itself with this external field. Thus the rotor will precess off its correct

axis of rotation, and we will lose our desired inertial reference. The energy dissipated by the rotor in precessing will cause it to slow down. This source of error can be overcome by properly shielding the rotor from any external magnetic fields.

The electric supporting field can also cause spurious torques in the following manner. The field, if the distance between electrodes and rotor is small, acts at right angles to the surface. If the electrodes are placed symmetrically about the rotor their resultant force will act through the geometric center of the rotor. If the rotor is not perfect spherical, its center of gravity will not coincide with its geometric center. The support field will thereby cause a torque about the center of gravity of the rotor which in turn will cause the rotor to precess and again we will lose our desired inertial reference. With the gimballed arrangement this source of error is easily overcome by adjusting the positions of the electrodes so that their net force acts through the center of gravity of the rotor.

In the non-gimballed system this type of correction is not applicable because as the gyro case turns about the rotor these torques will change. In this system the outputs of the gyro photomicroscopes are fed to a computor. The computor calculates the corrections

necessary to offset the effects of these spurious support torques.

The third and not uncommon source of error is mass unbalance. This source of error is best corrected by perfecting the manufacturing process. One technique used is to lap (add material in thin layers) to the heavy side of the rotor. The rotor is then remachined into a sphere so that its center of gravity moves towards its geometric center.

2.12 Conclusion

The Electrostatic Gyro is the first of the unconventional gyros to reach a state of development where it is being considered for operational use. An airborne navigational system is under development by Honeywell using ESG's. The United States Navy is also planning on using ESG's in its Polaris program (6).

One of the disadvantages of the ESG is the requirement for an extremely dependable support power supply. Even momentary loss of power results in the spinning rotor falling and literally destroying itself and its support. There is also the requirement for an extremely low vacuum which although easily obtained in the laboratory is not easily achieved when the device is operational.

In return for these disadvantages the ESG is reported to have a drift rate one or two orders of magnitude

better than conventional gyros.(5). The requirement on accuracy in gyros is rising to such an extent that conventional gyros can no longer be expected to meet it. The Electrostatic Gyro has the potential to provide this necessary accuracy.

CHAPTER 3

CRYOGENIC GYRO

3.1 Introduction

In the previous chapter it was pointed out that one of the limitations of convential gyros was their suspension system and that a field support provided a method of overcoming some of the inherent defects in bearing suspensions.

The Electrostatic Gyro used an electric field suspension system. The other known type of field support is magnetic. Under normal operating conditions magnetic suspension suffers from as many defects as does normal contact suspension. In order to provide the required support the magnetic field used for suspension must enter the body being supported. As a result energy is dissipated in the body in the form of eddy current and hysteresis losses. These losses in turn cause drift torques. If some means of support using magnetic fields could be devised such that it is not necessary for the supporting field to enter the structure, these sources of drift would not exist. The Cryogenic Gyro is built

around such a system.

The cryogenic gyro, like the electrostatic gyro, uses a sphere for its rotor. Unlike the electrostatic gyro, however, the cryogenic gyro's spherical rotor is supercooled so that it becomes a superconductor. Use is made of the fact that magnetic flux cannot enter a superconductor. This phenomena is called the Meissner effect. Using this phenomena we are able to support the cryogenic sphere with a magnetic field without fear of eddy current and hysteresis losses.

In the presentation to follow electric and magnetic properties of superconductors are discussed. In view of the fact that magnetic suspension is one of our aims in this gyro, the equation for the force exerted on a superconductor by a magnetic field is derived. Subsequent to this theory an outline of the physical characteristics of a representative cryogenic gyro is presented.

3.2 Superconductivity (1)

"Superconductivity" is the complete absence of electrical resistance in a substance. This word was coined in 1908 by Kammerlingh Onnes. Onnes had been carrying out experiments at extremely low temperatures on the resistance of metals. It had been known for some time that the resistance of metals decreased with temperature. However, because of the difficulty of achiev-

ing low temperatures, it was not known just how low this resistance became.

Onnes in 1908 successfully liquified helium and then was able to produce temperatures as low as $4.2^{\circ}K$ ($-268.8^{\circ}C$). With this ability he conducted experiments on the resistivity of metals, in particular, gold and platinum. It was found that these metals did not have zero resistance at $4.2^{\circ}K$. It was also observed that the actual resistance varied with specimens and appeared dependent on their impurity content. Onnes decided to use mercury which was the only metal which he could obtain with a high degree of purity. When the mercury was cooled to $4.2^{\circ}K$. Onnes found that the resistance had reached zero. He referred to this phenomena as "superconductivity".

Subsequent experiments revealed that the transition from a state of finite resistance to one of zero resistance occured very sharply at a particular temperature, known as the "transition" temperature. In spite of his earlier experience with gold and platinum, Onnes found that even when he added impurities to mercury, its resistance still went to zero. The change in resistance at the transition temperature, however, was not as sharp as before but instead tended to spread out.

With more experiments in the field, it has been found that twenty-one metallic elements, as well as

some alloys, become superconductors at a particular temperature. The transition temperature appears to be a characteristic of the material and varies from metal to metal. For example, the transition temperature of Halfnium is 0.35°K while for Niobium it is 8.0°K. Some alloys have even higher transition temperatures which have been found to be as high as 19°K.

At this particular time there appear to be no hard and fast rules to ensure that a particular substance will become superconductive although most materials with this property seem clustered in two separate areas in the Periodic Table. Also, since it is impossible to reach absolute zero, there may be other metals that become superconductive.

Later it will be seen that the metal that is utilized in the cryogenic gyro will be subjected to magnetic fields. At this point it is, therefore, worthwhile to point out the effects of magnetic fields on the superconductivity of metals.

Onnes in 1914 discovered that if a magnetic field were applied parallel to a superconductor, the resistance of the specimen returned to a finite value at a particular value of magnetic field, i.e., the specimen was no longer superconducting. This value of magnetic field became known as the "critical field" and, as with the transition temperature, varied with the particular metal.

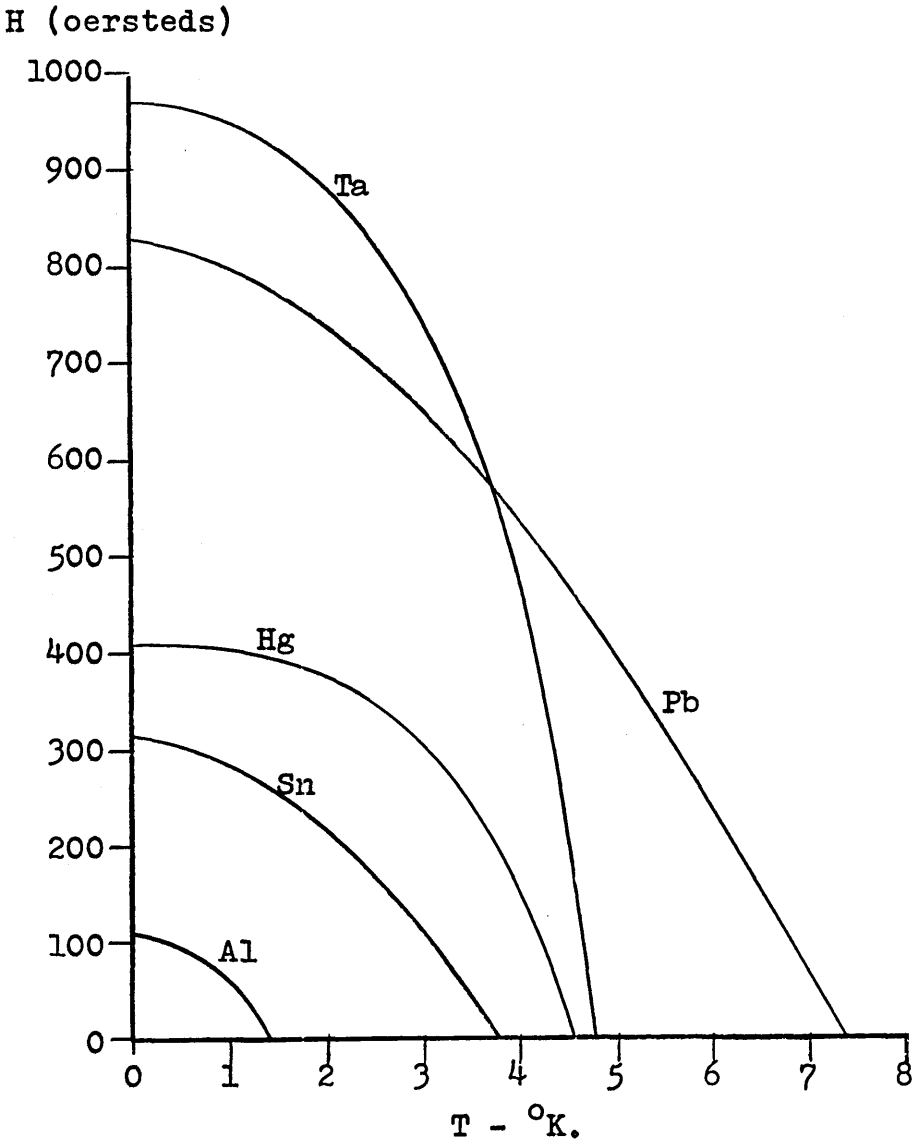

FIGURE 3-1

CRITICAL FIELD VERSUS TEMPERATURE

FOR SUPERCONDUCTORS

Figure 3-1 shows curves of critical field of intensity H versus temperature T for a number of representative metals. The region of superconductivity is the region to the left of the curve. It can be seen that the "critical field" varies with the metal, its temperature, and also (not shown in the figure) with any impurities in the material. If the impurities are localized in a specimen, the critical field will vary for various parts of the specimen. Later experiments have indicated that the initial slope of the H vs T curves for "soft" metals is less than for "hard" metals. (The expressions "soft" and "hard" refer to the relative melting points of the metals, the melting point of "hard" metals being higher than that of "soft" metals.) Also the low slope for the soft metals has revealed itself in a variance of critical field for the same specimen.

The size of a specimen can also effect its superconducting properties, but the size of material found in cryogenic gyros will be large enough that this effect can be ignored.

3.3 Magnetic Properties of Superconductors (1)

For a number of years after the discovery of superconductivity it was assumed that the magnetic properties of superconductors could be deduced from their superconducting properties. That is, if a magnetic field existed in the region before a metal was super-

cooled, then once the metal had reached its superconducting state the field inside the specimen would remain. The theory being that a metal having zero resistance would not cause the internal field to decay.

In 1933, Meissner and Ochenfield, while carrying out experiments on the magnetic properties of superconductors, found this theory to be false. Instead, they discovered that the field distribution around a superconductor was of such a nature that zero field existed inside the superconductor. To put it simply, when a metal, which is located in a magnetic field, is cooled so that the surrounding field is below critical, the metal will expel the field entirely from its interior. This phenomena of a superconducting body expelling a magnetic field is known as the Meissner Effect.

3.4 Force of a Magnetic Field on a Superconductor (2)

Having looked at the electric and magnetic properties of superconductors we are now in a position to show that a magnetic field exerts a force on a superconducting body.

Basic electric theory tells us that if a wire of unit length with current I flowing in it is placed in the vicinity of and normal to a magnetic field whose flux density is B, a force will be exerted on the wire by the magnetic field that is

$$F = BI \qquad (3.1)$$

Hence, in order to have a force of magnetic origin it is necessary to have current flow. We will see that the Meissner effect can be explained by assuming that a current exists on the surface of a superconductor. This current is proportional to the strength of the external field surrounding it. To understand this idea the following is presented.

Let us consider a metal plate with a wire adjacent to it (Figure 3-2a). The plane of the plate and the axis of the wire are both normal to the page. If a DC current is made to flow through the wire, a field will build up around the wire and enter the plate. As this field enters the plate, it will induce currents in it. These currents will be normal to the paper as is the current in the wire but will be opposite in direction in accordance with Lenz's Law. These induced currents in turn will produce a magnetic field that will tend to cancel the applied field inside the plate. At normal temperatures the plate has resistance and therefore these induced currents will decay with time. Once these currents have decayed, the field produced by the current in the wire will enter the plate as is shown in Figure 3-2a.

Let us now put an AC current through the wire. The external field will oscillate radially about the wire. If these oscillations are of sufficently low frequency,

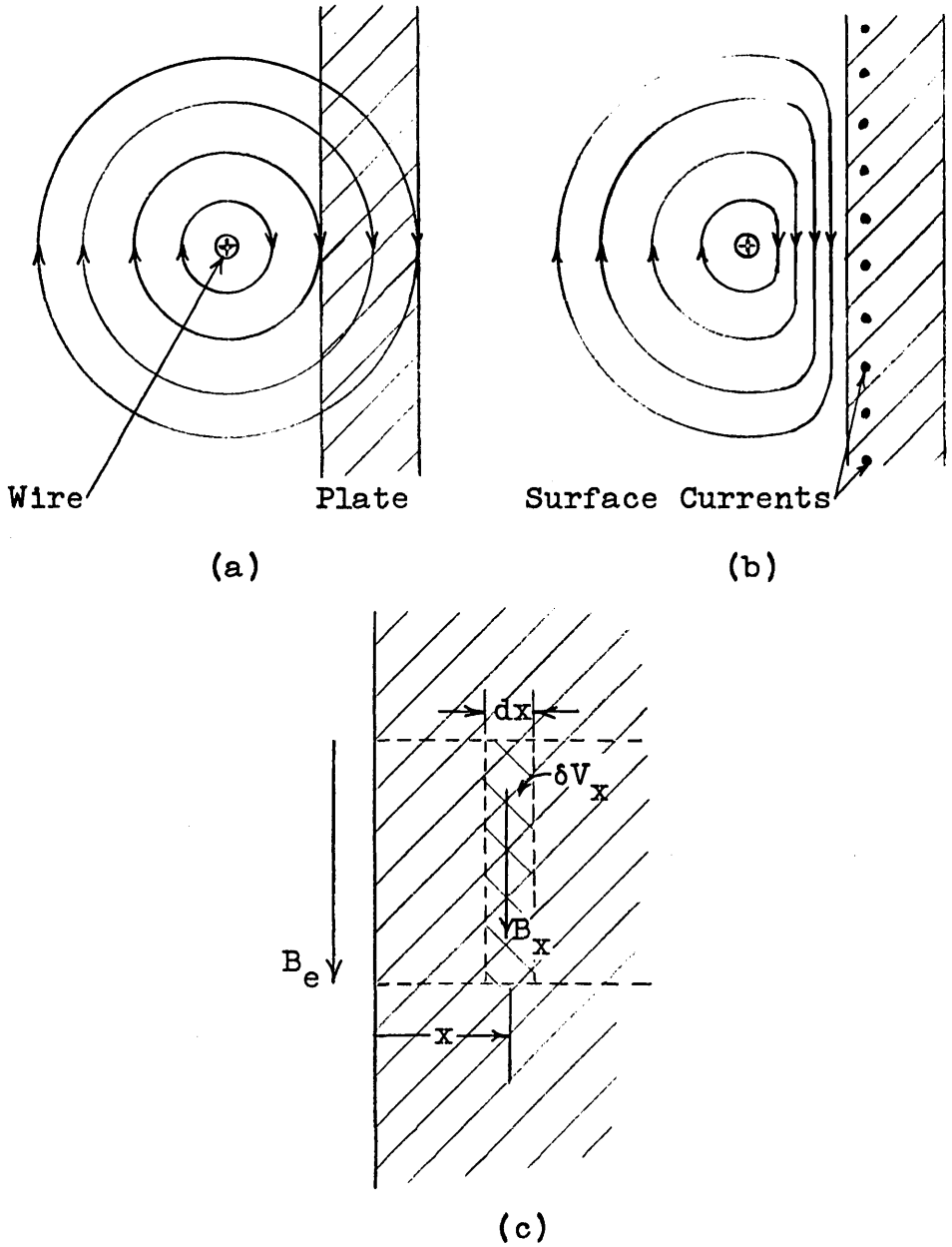

FIGURE 3-2

MAGNETIC FIELD AROUND A METAL PLATE

(a) AT NORMAL TEMPERATURE; (b) AND (c) SUPERCONDUCTING

a condition almost identical to the DC case will result, because the time required for the induced currents in the plate to decay will be less than 1/2 the period of the AC current in the wire. As the frequency of the AC current in the wire increases, the period of the oscillations will become less than the decay time of the induced currents in the plate. This means that the field produced by these induced currents will not completely decay but will cancel some of the externally applied field inside the plate, at the same time reinforcing the field outside the plate. If the frequency of the AC current in the wire is made high enough, a condition will exist whereby the induced currents do not decay; and the field produced by them will completely cancel the externally applied field inside the plate while simultaneously reinforcing the external field outside the plate. In actual fact the induced currents exist only in a region very near the surface of the plate. If the thickness of the plate is much larger than the depth of the region in which these induced currents exist, the condition can be considered identical to one where the external field does not enter the plate at all. If the plate is made superconducting and the external field is DC, we can see that the condition is analagous to the Meissner effect. In actual fact the currents in the surface of a superconducting plate

resulting from an externally applied field exist to a depth of about 10^{-4}mm (2). Having established a current in the surface of a superconductor, we are now in a position to use Equation (3.1) to derive the force of a magnetic field on a superconductor.

Refer to Figure 3-2c which is a magnified view of the edge of a plate; i.e., the surface of the plate is normal to the paper. We now wish to find the force on a unit area of the surface. Using Equation (3.1) the elemental force is

$$\delta F = B_x \delta i_x$$

where B_x is the magnetic flux density at a distance x measured from the surface of the plate, and δi_x is the current in the volume δV_x (Figure 3-2c). The total force on the unit area is therefore

$$F = \int_{x=o}^{x=\infty} B_x di_x$$

Integrating by parts gives

$$F = \left[B_x i_x - \int i_x dB_x\right]_{x=o}^{x=\infty} \qquad (3.2)$$

The first term on the right vanishes because $i_o=0$ ($V_x=0$ when x=0) and $B_\infty=0$. Integration of the second term requires i_x in terms of B_x.

Maxwell's Law states that the total current i in the region near the surface, i.e., the total current to

the right of the surface edge in Figure 3-2c, is

$$i = \frac{H_e}{4\pi}$$

where H_e is the external field intensity. Similarly, the current contained in the volume to the right of point x is

$$i_{x_o} = \frac{H_x}{4\pi}$$

where in this case H_x is the magnetic field intensity at x. Therefore, the current i_x, which is $i - i_{x_o}$, is

$$i_x = \frac{H_e - H_x}{4\pi}$$

Assuming unit permeability,

$$i_x = \frac{B_e - B_x}{4\pi}$$

Substituting in Equation (3.2) gives

$$F = -\frac{1}{4\pi}\int_{x=o}^{x=\infty}(B_e - B_x)dB_x$$

$$= -\frac{1}{4\pi}\left[B_e B_x - \frac{B_x^2}{2}\right]_{x=o}^{x=\infty}$$

Since $B_o = B_e$ and $B_\infty = 0$,

$$F = \frac{B_e^2}{8\pi} \qquad (3.3)$$

where F is the force per unit area on the plate due to an external field of flux density B_e. This force is a

force of repulsion; and because the flux lines are tangential to the surface (this follows from the fact that the flux lines do not enter the surface and therefore no component of flux can be normal to the surface), the force will be normal to the surface.

It has thus been established that a magnetic field exerts a force on a superconductor. Unlike the electrostatic gyro, however, this is a force of repulsion and the problems of stability associated with the electrostatic gyro are not present here.

3.5 The Cryogenic Gyro

Let us now examine a typical cryogenic gyro. For this purpose a design by General Electric Company has been chosen (3). It should be noted that this design has changed somewhat with development being carried out by General Electric under Project Spin for NASA. However, to illustrate the necessary details, Figure 3-3 has been extracted from reference (3). The discussion will be broken down as follows:

(1) General environmental requirements.

(2) The rotor and the requirements on its geometry.

(3) The suspension system with its limitations.

(4) Spinning of the rotor.

(5) Gyro readout and alignment.

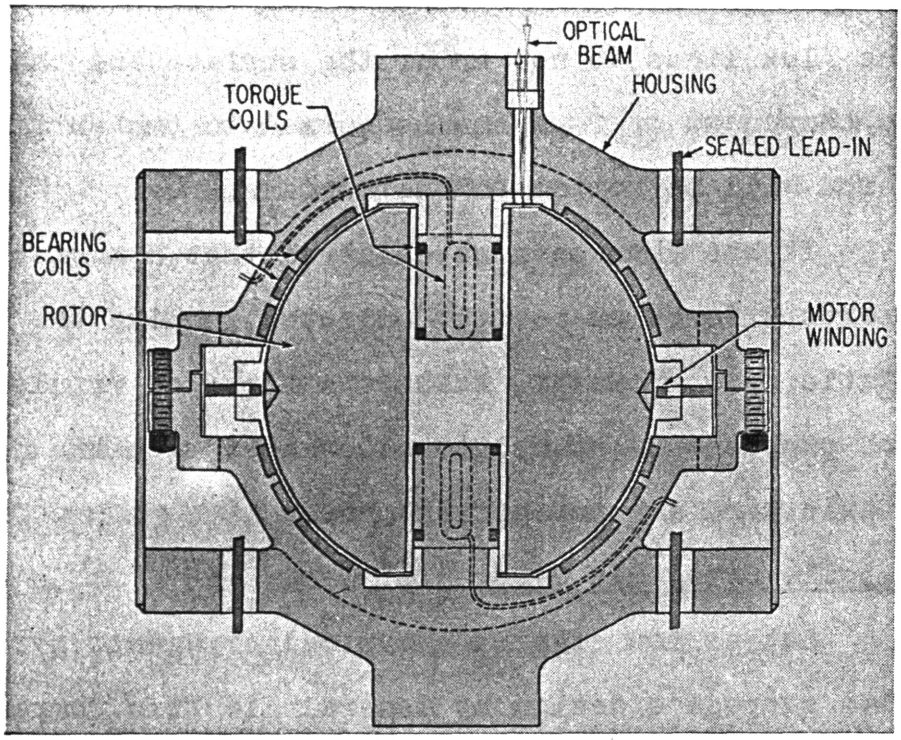

FIGURE 3-3

CYROGENIC GYRO

(Figure Courtesy of Missiles and Rockets)

3.6 Environment

The most obvious requirement on environment follows from the theory presented in Section 3.2 in that extremely low temperatures are necessary. In the laboratory this is quite easily accomplished with a supply of liquid helium. When the gyro is made operational, however, this will not be quite so simple. In the first place, because of weight limitations in most inertial applications, a large supply of reserve helium will make the cryogenic gyro too bulky and heavy. It will, therefore, be necessary to provide adequate thermal shielding and to optimize the use of the liquid helium supply.

To reduce drag on the rotor when it is spinning, the case is evacuated. Unlike the ESG, however, the supporting field arrangement does not place rigid requirements on the level of vacuum.

3.7 Gyro Rotor

As with the ESG the supporting field produces a force normal to the surface of the body being supported. Thus, in order that the supporting field produce no torques on the gyro rotor, a spherical rotor is the best design.

As will be seen in Section 3.9, one method proposed to bring the rotor up to speed places indentations on the surface of the rotor. These indentations destroy

the sphericity of the rotor; and if they are not placed symmetrical about the rotor, the supporting field will produce a torque on the rotor. One method of overcoming possible torques due to the indentations is to shield these indentations from the supporting field. This shielding, however, is not perfect but can keep the drift down below a desired level.

If the rotor, when it is supercooled, is located in a magnetic field, the field is expelled (Section 3.3). However, should strains or impuritiies be present in the material, this expelled flux will become trapped in the areas containing the impurities. This trapped flux will react with the supporting field and produce unwanted torques (4). Torques caused by trapped flux can be reduced by supercooling the sphere in a field-free atmosphere. This also is not perfect but can keep errors below an acceptable level.

3.8 Field Support of the Gyro

In order to support the sphere, some method of producing a magnetic field must be devised. Conceivably, permanent magnets placed around the periphery of the sphere could produce the necessary field. With this method, however, it would be difficult to obtain a symmetrical distribution of flux; and areas of excessive flux, possibly even above critical (Section 3.2), could result.

An alternate method, making use of the superconducting properties of metals, is to surround the sphere with supercooled rings. Current in these rings will produce a magnetic field. Once current is established in the rings, the source can be removed; and because of the zero resistivity of the rings, the current will not decay.

One consideration that must be kept in mind when designing a supporting field system is that the field must not exceed the critical value anywhere on the sphere. If this happens, superconductivity at that point will be destroyed. Jet Propulsion Laboratories (5) carried out a study by computer to determine the optimum arrangement of coils to support a sphere. They found that six coils whose planes were perpendicular to the local vertical and also equidistant from each other were equally effective in producing support as were an infinite number. Also it was found that for maximum force on the ball, coil sphere diameter to rotor diameter of 20 was optimum (5). General Electric (3) in the design of their gyro utilize 6 coils (Figure 3-3). They, however, do not use optimum coil sphere diameter to rotor diameter. JPL also indicate that they have supported a 300 gram niobium sphere under a force of 1g (3).

3.9 Bringing Up to Speed

Having supported the rotor it is now necessary to

rotate the rotor at sufficient speed to produce the necessary angular momentum. It would appear that the easiest method would be to surround the sphere with a rotating field and bring the sphere up to speed by induction. This method will not work. As has already been pointed out in Section 3.3 the field will not penetrate the ball once it is supercooled. As was seen in Chapter 2, to achieve rotation by induction, the field must penetrate the ball.

One technique used is to place a series of concentric indentations around the equator of the sphere. A stator consisting of two superconducting loops is placed in the equatorial plane of the rotor. These loops have projections that extend toward the rotor. The number of projections on each loop equals the number of indentations on the rotor. The two loops are slightly displaced with respect to each other. By properly pulsing these loops alternately, it is possible to rotate the rotor ball and to bring it up to speed. As has already been mentioned the possible difficulty with this method is that once the ball is up to speed, these indentations, which are no longer required, could react with the supporting field and produce unwanted torques if adequate shielding is not provided.

Another method which does not require indentations on the rotor is to use helium jets directed at an angle

to the surface of the rotor. Once the ball has been brought up to speed, the enclosure can be evacuated to reduce drag on the ball. JPL reports (5) that it was possible to spin a rotor up to 7000 RPM with this method.

3.10 Read Out and Alignment

In the General Electric design, read out is accomplished by placing a mirrored surface on the pole of the rotor sphere. Optical readouts detect rotation of the rotor (Figure 3-3). In this design, these misalignment signals are used to rotate the rotor rather than to align the case with the rotor.

Torque coils are placed in the core of the rotor (Figure 3-3). Currents proportional to the angular rotation of the rotor sphere are fed to these coils. The fields produced by the coils react against the rotor core re-centering the rotor. Possible difficulties with this method result from two sources. First, the presence of the core in the rotor destroys the sphericity. As has been pointed out before, the support field could cause undesired torques because of this. Secondly, we have the possibility of "trapped" flux. It will be recalled that when the ball is supercooled, it expells any flux that was contained within it before it was supercooled. Thus, it is possible, unless the ball was adequately shielded when it was supercooled, that a quantity of flux would be trapped in the core. This

flux could react with the support field and produce drift of the rotor. Shielding of the rotor core from the support field aids in overcoming these possible errors.

3.11 Conclusion

The Cryogenic Gyro represents another application of field support. Unlike its contemporary, the ESG, it has not reached the stage of development where it can be considered for operational use. The difficulties of the design have been pointed out in the previous sections. If the gyro is to be considered for long term application where size limitations are present, the greatest drawback is the requirement for the extremely cold environment.

General Electric Company is presently carrying out development work on the cryogenic gyro under Project "Spin" for the National Aeronautics and Space Administration. It will be interesting to see the results of this project to see if it is possible to utilize this gyro as a replacement for existing conventional types in long term applications.

CHAPTER 4

LASER GYRO

4.1 Introduction

For many years, scientists have been dreaming of and looking for a source of coherent light. It was first achieved in 1960, and in 1963 this "new light" was being used to sense and measure inertial rotations. It is the property of coherence at high frequencies that makes the detection of small rates possible.

A brief description of this application is as follows. See Figure 4-1. Two beams of light are caused to traverse a closed loop - one beam clockwise; the other, counter clockwise. At some point along the periphery of this loop, the two beams are sampled and their frequencies compared. If the entire assembly is not rotating with respect to inertial space, then the two beams will be of identical frequency and their difference in frequency zero. If the assembly is rotating about an axis perpendicular to the plane of the loop, then one beam, the one with the rotation, must travel farther than it did before to reach the sampling

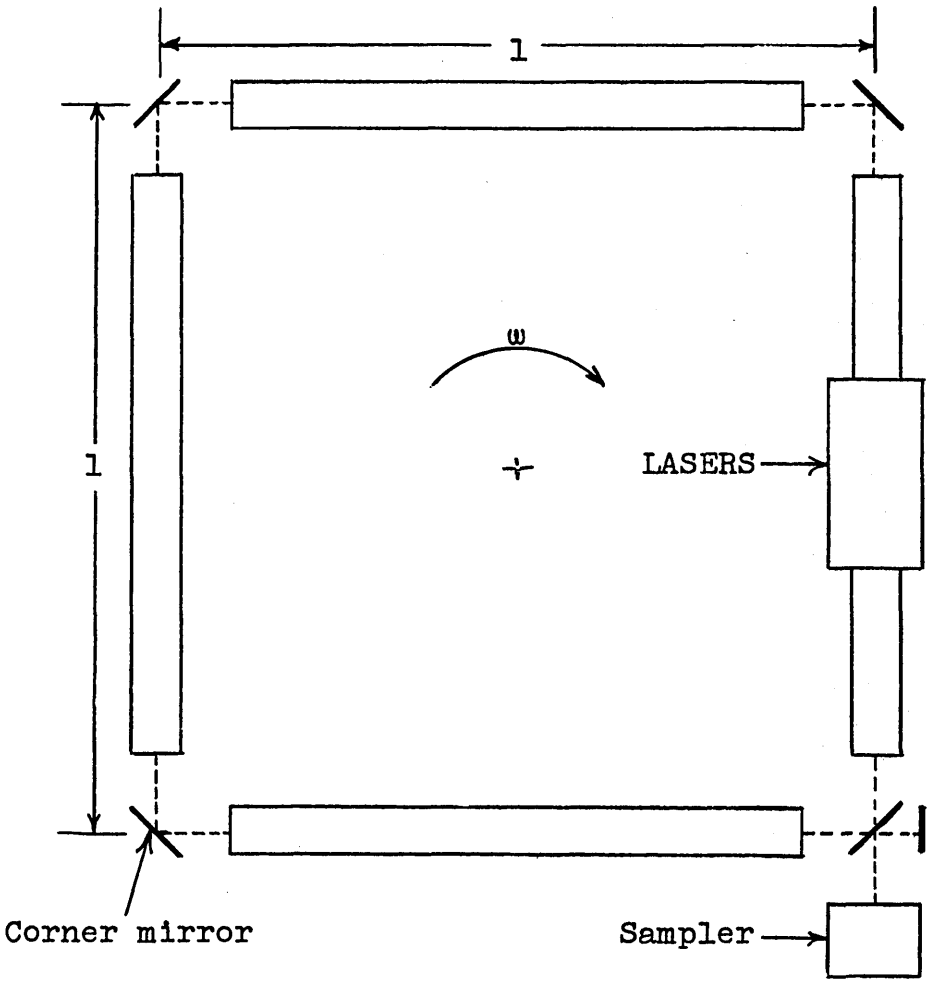

FIGURE 4-1

LASER GYRO

point while the other travels a lesser distance than it did previously. This difference in travel distance is analagous to an apparent shift in frequency via the well understood Doppler effect. Hence, the difference in the sampled frequencies of the two beams is a measure of inertial rotation.

Earlier experiments have been conducted in the study of the effects of rotation on the propagation of light including the observation of inertial rotation. These earlier experiments include those of Harress in 1911, of Sagnac in 1913, and those of Michelson and Gale in 1924. Having only non-coherent light sources available, all were forced to rely on interference fringe patterns for determinations. And in order to obtain measurable fringe shifts, either high rotation rates or extremely long optical path lengths were necessary. In contrast, the property of coherence associated with laser light has enabled the use of more accurate and convenient Doppler shift measurements.

4.2 Basic Derivations

Two questions immediately come to mind. First, why hasn't the Doppler effect been used in this application before? And second, since the whole assembly is rotating, there is no relative velocity between the source and the sampler. Hence, how can the Doppler effect occur?

The answer to the first question is "It could have

been" if we had the capability to measure a difference in frequency of microcycle-per-second magnitude between two frequencies at 10,000 megacycles for each meru (milli-earth-rate-unit) of sensing capability desired. Of course, the stability of the 10,000 mc signal generator would have to be orders of magnitude better than the difference frequency to be observed. The mathematics for this example will be developed later in this section.

The second question is a little more difficult to answer. The Doppler effect is the apparent shift in frequency arising from relative motion along the path of propagation between the transmitter and receiver. It assumes the constancy of the speed of light. Yet in our application, we observe a frequency shift with no relative motion along the path of propagation. Is the speed of light no longer constant to and invarient among observers?

Landau and Lifshitz (1) treat the problem of non-inertial frames of reference. They conclude that the speed of light is indeed constant for inertial observers but appears to change for non-inertial observers, in particular, rotating observers.

Their investigation concerned the propagation of light in a closed loop. The shape of the loop was neither specified nor implied and is in fact immaterial. The

following is a summary of their analysis.

The difference in transit time for their beam from that with no rotation is given as

$$\delta t = \frac{1}{c^2}\int \frac{\omega r^2 d\phi}{1-\left(\frac{\omega r}{c}\right)^2}$$

$$= \frac{\omega}{c^2}\int r^2 d\phi$$

$$= \pm \frac{2\omega A}{c^2}$$

where δt = transit time difference
c = speed of light
$\omega = \dot{\phi}$ = angular velocity of the loop
r = radius of the loop
A = area of loop projected on a plane normal to the axis of rotation.

Notice the assumption that $\omega r/c$ is much less than 1. This is mathematically sound for our application.

If the circumference of the loop is L, the actual time of transit is given as

$$t = \frac{L}{c} \pm \frac{2\omega A}{c^2}$$

$$= \frac{L}{c^2}\left(c \pm \frac{2\omega A}{L}\right)$$

Hence, they conclude that the speed of light appears to be given as

$$c_{app} = c \pm 2\omega\frac{A}{L}$$

Let us apply this result to determine the frequency shift of our two beams of light.

$$f_1 = \frac{c_{app}}{\lambda} = \frac{c-2\omega\frac{A}{L}}{\lambda}$$

$$f_2 = \frac{c_{app}}{\lambda} = \frac{c+2\omega\frac{A}{L}}{\lambda}$$

where f_1 and f_2 are the observed frequencies of the beams traveling with and opposite to, respectively, the rotation of Figure 4-1; and λ is the wavelength. The frequency difference $f_2 - f_1$ is therefore

$$\delta f = \frac{4\omega A}{\lambda L} = \frac{4Af_s}{cL}\omega \qquad (4.1)$$

where f_s is the frequency of the light source; other symbols, as previously defined. Equation (4.1) is the basic equation for our application. Note that this derivation assumes that the two beams are actually of identical frequency (same λ) but only <u>appear</u> to have different frequencies. More will be said on this point in Section 4.6.

Using this relationship, the geometry of Figure 4-1 with each side one meter in length, and a source frequency of 10,000 mc as in the earlier example, we find

$$\delta f = \frac{10^{10}}{3x10^{8}}\ 7.26x10^{-8}$$

$$= 2.42x10^{-6}\ \text{cps}$$

as the observed difference frequency for each meru of angular velocity input.

It is interesting to note that the fundamental relationship of Equation (4.1) can be derived from a

non-relativistic analysis. Consider the case of a fixed transmitter/receiver and a target moving relative to it at a distance d. In time interval δt, the distance d changes by δd. The signal as received at the target has its phase shifted relative to what was transmitted by an amount

$$\frac{\delta d}{\lambda} = \text{number of wavelengths out of phase}$$

$$\delta\phi_{target} = 2\pi\frac{\delta d}{\lambda} \text{ radians}$$

$$\delta\phi_{rcvr} = 2x2\pi\frac{\delta d}{\lambda} \text{ radians}$$

From which we get

$$\begin{aligned} \delta f &= f - f_o \\ &= \frac{1}{2\pi}(\omega_o + \frac{\delta\phi}{\delta t} - \omega_o) \\ &= \frac{2}{\lambda}\frac{\delta d}{\delta t} \\ &= \frac{2}{\lambda} v_r \end{aligned} \qquad (4.2)$$

where v_r is defined as $\delta d/\delta t$ (2).

In our application, the receiver is separated from the transmitter and the path can be considered "one way". But we have a beam going in both directions each of which is shifted an equal amount; hence, the factor of 2 in Equation (4.2) stands.

In order to apply Equation (4.2), it is necessary to think of v_r as the component in the direction of propagation of the velocity of the receiver relative to

that point where the transmitter was when the wave was emitted. For the situation in Figure 4-1, that would be the product of some radius and the angular velocity. But what radius? Casual inspection of Figure 4-1 would suggest $l\sqrt{2}/2$, the semi-diagonal. Further investigation will show this to be incorrect.

Consider for a moment any regular planar polygon having n sides each of length l. Let r be the radius of the inscribed circle. Reference to any mathematical tables will reveal the following relationships.

$$\text{Area} = A = \frac{1}{4}nl^2\cot\frac{180^\circ}{n}$$

$$\text{Perimeter} = L = nl$$

$$r = \frac{l}{2}\cot\frac{180^\circ}{n}$$

And from these relationships comes another:

$$r = \frac{2A}{L}$$

If this radius is used in Equation (4.2), it becomes equivalent to Equation (4.1).

$$\delta f = \frac{2v_r}{\lambda} = \frac{2(\text{radius})}{\lambda}\omega$$

$$= \frac{4A}{\lambda L}\omega$$

Hence, the proper radius is that of the inscribed circle.

4.3 Coherence

At the outset it was stated that it was the property of coherence that makes all this possible. It is

here that the word LASER enters the picture. For it is the laser that has given scientists their first source of coherent light.

Coherence (3) can best be defined in terms of correlation functions. An electromagnetic wave may be either spatially coherent or time coherent or both. A wave is said to be spatially coherent if a time correlation can be found (or is known to exist) between the magnitude of the wave at any two points on a plane perpendicular to the direction of travel of the wave. A wave is time coherent if a time average auto-correlation function exists. For our purposes, the following statement about coherence will suffice. The extent to which a wave approaches a single frequency is a measure of time coherence.

A byproduct of coherence is that the beam width of focused light is governed by the laws of diffraction rather than by the size of the source as we are accustomed to think. With sufficiently precise optics, fractional arcsec beam widths should be attainable.

With the definition of coherence, it is immediately apparent that in order to observe a Doppler effect, the signal source must produce time coherent radiation. Ordinary light, being incoherent, is not suitable for our application. But from Equation (4.1), we see that higher frequencies are desirable from sensitivity con-

siderations. Light, if coherent, being four orders of magnitude higher in frequency than that of microwaves, is decidedly advantageous.

4.4 MASER Background

The letters comprising the word LASER stand for Light Amplification by Stimulating Emitted Radiation. The name and the device itself are follow-ons from the MASER where M stands for Microwave. It is therefore logical to begin with the MASER. It should be stated that the primary difference between MASERS and LASERS is the frequency, or, alternatively, wavelength, of the emitted radiation. In the discussion to follow, an acquaintance with elementary quantum physics is assumed.

Briefly in review, these points (4) need to be remembered. Shortly after the discovery of the electron by Thomson (1897), Zeeman and Lorentz proved that the electron participated in the emission of spectral radiation. Planck quantized the energy levels. Einstein, in 1905, quantized the radiated field itself (i.e., energy can be absorbed from it only in quanta of size hf, where h = Planck's constant and f = frequency). And Niels Bohr, in 1913, theorized these statements among others:

1. Radiation is emitted whenever the atom jumps from one allowed energy state E_2 to a lower state E_1.

2. The frequency of radiation is determined by the "Einstein frequency condition": $hf = E_2 - E_1$. Previous investigation had shown that an atom could be "excited" or "pumped" into higher energy states. If the exciting or pumping energy is electromagnetic in nature, its frequency must also satisfy the Einstein frequency condition.

In order to clarify the range of frequencies involved and to view them in perspective, the following table is presented:

FM Broadcast		10^8 cps	
UHF TV (max)		10^9 cps	
Microwave Band	10^9 -	10^{11} cps	] maser
Not used	10^{11} -	10^{12} cps	
Infrared	10^{12} -	5×10^{14} cps	] laser
Visable Light	5×10^{14} -	8×10^{14} cps	
Ultraviolet	8×10^{14} -	10^{17} +cps	
X Rays	10^{17} -	10^{20} +cps	
Gamma Rays	10^{20} -	cps	

The maser is a quantum electronic device that uses the atoms of molecules in matter as reservoirs for energy. This energy is then recaptured or released in the form of photons, packets of electromagnetic energy.

The devices are of two types, solid-state and gaseous. Of the solid-state masers, most require cooling to temperatures approaching absolute zero; some yield

pulsed outputs; and none are as nearly monochromatic, or frequency stable, as are the gaseous types (3). An additional advantage of the gaseous type will be brought out later.

The basic principles of maser amplification are well presented by Brinley (5). The following is based primarily on his article. First, a choice of material must be made. The material must be such that under suitable conditions it can be excited to two different energy levels, E_2 and E_3, above that of its ground state E_1. The key requirement is that the energy difference $E_2 - E_1$ correspond via the Einstein frequency condition to the frequency to be amplified.

Typically, a ruby crystal is involved because of its atomic structure and susceptibility to excitation with the proper energy level separations. It is cooled to near zero degrees absolute temperature in order to at least partially vacate the outer electron orbits. An externally supplied magnetic field is then superimposed in the crystal's region for two reasons: to make the electrons more susceptible to excitation and, more importantly, to control or to determine the level of the excited states. The reason for this will be readily apparent shortly.

Let us now refer to the non-excited and supercooled state as the ground state and to the outer elec-

tron orbit thereof as the n=1 level. Further, let us refer to the energy associated with an electron in the n=1 level as E_1.

The ruby crystal is then subjected to excitation which excites, or "pumps", electrons all the way to the n=3 level. Note here that in accordance with the Einstein frequency condition, the pump frequency is determined by the energy difference $E_3 - E_1$. The "excited" electrons now fall back spontaneously from the unstable n=3 orbit to a momentarily (as long as one second) stable n=2 orbit.

No mention is made at this point about what happens to the energy released in this first and spontaneous decay transition. Further, no mention of or reference to amplification has yet been made.

A second electromagnetic wave, the one to be amplified, now enters and <u>stimulates</u> the second and final decay transition of the electron from the n=2 to the n=1 level. The energy difference $E_2 - E_1$ corresponds as previously noted to the frequency to be amplified. It is the absorbtion by the wave of this <u>stimulated</u> emission that constitutes amplification.

Note that there are two transitions involved. one is spontaneous whereas the other is stimulated. Note also that since the energy difference $E_3 - E_1$ is greater than $E_2 - E_1$, it follows that the pump frequency

must be higher than that of the signal to be amplified.

Since the position of a particular electron within the crystal lattice determines the internal magnetic field it sees, the total magnetic field varies for the various electrons. In view of the fact that the total magnetic field in part determines the various energy levels, it follows that the various excited electrons will respond to different incoming frequencies. The gaseous maser, by the very fact that its medium is a gas, has a more nearly uniform internal magnetic field. It therefore follows that the solid-state maser has a broader bandwidth than does its gaseous counterpart.

In regard to the energy released during the spontaneous transition (from n=3 to n=2) it is released as noise radiation. It can now be seen that the element to be used as the heart of a maser must be chosen judiciously for the frequencies involved must be mutually non-interfering. External magnetic fields can pull the operating frequencies somewhat but at the expense of stability margin.

The original ammonia maser was first operated in 1955 by Dr. Townes of Columbia University. The frequency stability was one part in 10^{11} (5). A hydrogen maser was operated in late 1960 by Prof. Ramsey at Harvard achieving a stability of one part in 10^{15} (5). It is interesting to note that a ruby maser is used as the

first stage of amplification in the receiver at Earth Station Number 1, Andover, Maine, the Telstar communications facility of Bell Labs.

4.5 LASER Operation

The laser operates much the same as does its forerunner, the maser. Operation to date of the laser has been one of generation rather than of amplification - the generation of coherant light. The atoms of some medium are excited. The radiation that results from the decay transitions is in or close to what is known as the visible light portion of the electromagnetic spectrum. But at this point the decay transitions are spontaneous and the light emitted is as yet incoherent (6). The radiation of incoherent light must occur in a resonant cavity in order to obtain coherent radiation.

A cylindrical tube-type cavity will be resonant if it is an integral number of half-wavelengths long. At each end of such a tube, a mirror is precisely positioned. It should be noted that at 10^{14} cps a wavelength is approximately 10^{-4} inches. Some of the omnidirectional incoherent light is repeatedly reflected within the tube and subsequently excites a resonant mode of the cavity. The associated field stimulates additional emission which is phase or time coherent (6). It is through this process that coherent light may be generated.

The first laser was operated in June 1960 by T. H. Maiman at Hughes. Its output was pulsed in that the stimulated transitions could not be continuously sustained. The first continuous wave (CW) laser was operated by Ali Javan of Bell Labs in January 1961. It is a gaseous CW laser that has been used by Sperry to sense inertial rotations.

The gaseous medium is a mixture of helium and neon. The helium atoms are excited by a relatively low-frequency and readily available 28 mc current. The energy stored in the excited helium atoms is transferred to the neon atoms through collisions. The incoherent light radiation occurs from the neon decay transition. Subsequent buildup of the coherent wave is as before. Coherent CW outpower is approximately 20 milliwatts (6). A report by Javan, Ballik, and Bond of Bell Labs (7) reveals an attained stability of less than 2 cps for several seconds which was slightly better than one part in 10^{14}. Line widths (frequency stability) of 1 cps have been reported (6). Approximate power input at 28 mc is 100 watts. And very important is the fact that this gaseous laser operates at a "room temperature" of $80^{\circ}F$ (3).

An additional advantage of the gaseous laser over its solid-state counterpart is the fact that it is less susceptible to multi-moding, the generation of more

than one frequency. As many as 10 modes is not uncommon in the solid—state version whereas only 2 or 3 may be present in the gaseous laser (3).

4.6 Application

In its Infrared/Optics/Laser Group, Sperry Gyroscope Company has been operating what it calls a Ring Laser Rotation Rate Sensor since January 1963. One configuration utilizes four CW helium-neon lasers arranged to form a square ring, as in Figure 4-1, with each side one meter in length. Energy is radiated from both ends of all four lasers. At each corner a mirror is positioned at a 45 degree angle such that light emitted from one laser is reflected into the next one. Hence, the cavity length is the entire periphery; and two beams are traversing the ring in opposite directions. One of the four corner mirrors is only thinly silvered and permits a portion of the energy of both beams to pass through it. The sampled beams are combined in a photo-multiplier tube and through the convential process of heterodyning, a beat note equal to the difference in frequency of the two beams is obtained.

In the absence of inertial rotation, the two beams are of equal frequency as before. But in the presence of rotation, two conventions of thought prevail. The second is more proper. The first says that the emit-

ted radiation is of constant frequency. The observed frequency would differ as previously explained. This point of view is substantiated via the Einstein frequency condition and the "constant" energy difference between the excited and ground state levels of the neon atoms. The other point of view is somewhat contradictory in that it argues that the two beams are actually of different frequencies. This latter point of view finds its validity in the fact that the cavity must be resonant, i.e., an integral number of half-wavelengths long, for coherent light generation and in the fact that the two beams must travel slightly different lengths to return to their respective starting points. Hence, the cavity is resonant at different frequencies for the two beams. Both points of view yield the same result, namely Equation (4.1), the basic equation of our application.

One Sperry experiment has a source frequency of 2.6×10^{14} cps or a wavelength of 1.153 microns (8). Inverting Equation (4.1) and substituting Sperry parameters yields

$$\omega = 1.153 \times 10^{-6} (\delta f) \quad \text{rad/sec}$$

In May 1963, the difference frequency (δf) detection threshold was down to 80 cps (9). This yields an angular velocity of 92.3×10^{-6} rad/sec or 1.27 times earth rate. When one considers that the device was first

operated only four months previous, this is indeed remarkable progress.

A later report from Dr. George White (10) in April 1964 indicates further substantial progress by Sperry. Only one laser is used and the geometry is that of a triangle rather than the previously used square arrangement. Inertial rate detection capability is now down to less than 1/10 earth rate or approximately 1.5 degrees/hour. The Sperry device now has a zero-rotation rate bias of about 1000 cps which enables determination of sense of rotation. The most recent Sperry version measures less than one foot across (11).

Only one report was found on work being done by Kearfott Division of General Precision Aerospace. It indicated a triangular arrangement with each side 54.5 inches long. They expect to be operational within two years with a detection capability of less than 0.001 degrees/hour (12).

4.7 Mossbauer Effect

Appropriate to this chapter on lasers is mention of the Mossbauer effect. With reference to Equation (4.1), the source frequency appears as a scaling constant. This is why light was advantageous over microwave sources. With reference to page 65, gamma rays are at least five orders of magnitude higher in frequency than light. Is there a source of coherent gamma rad-

iation? The Mossbauer effect is just that.

This discovery by Rudolph Mossbauer, an Austrian physicist, won him the Nobel prize in 1958. The coherence, or frequency stability, of the radiation is attributed to the no-recoil emission of the photon on the losing nuclei. If recoil existed, the losing nuclei would move during the emission process. This movement results in what is appropriately known as the Doppler broadening of the spectral line. Without this movement, i.e., no-recoil emission, the radiation is extremely coherent. Stability is reported as being on the order of 1 part in 10^{15}, extremely good (13).

4.8 Conclusions

As reported by Dr. White (9), no clearly fundamental limits had been encountered but the following difficulties were then present: the presence of more than one mode of oscillation and angular vibrations of the corner mirrors which amplitude modulated the beams. Another difficulty is the possibility of cross-coupling between the two beams (14).

Although the yet attained performance capability of the laser inertial rate sensor is still several orders of magnitude poorer than that of present day floated rate integrating gyros, there are several factors on the plus side. First and most important is the fact that the laser device contains no moving parts, the

major limitation of conventional inertial sensors. Second, and almost as important, is the fact that the laser device is almost totally immune to both gravity and linear acceleration of the vehicle containing it. Further, the stability of materials and the precision of machining are not first order considerations.

The output of the laser gyro is basically digital in nature as opposed to analog of the conventional gyroscope. Through a process of amplification, clipping, differentiating, and counting, instantaneous readout of both angular velocity and angular displacement is possible. Measurement of angular displacement to accuracies of tenths of arcseconds may be obtained in the near future (8).

Because the large dynamic range requirements result in excessive drift rates in conventional instruments, the laser gyro offers particular promise in strap-down inertial navigation systems. There is no inertia reaction from the laser gyro on a spacecraft that might be carrying it. The laser gyro offers no friction, indefinite life, and instantaneous warmup. Finally, the promise of improved sensitivity, long-term stability, and extremely low cost make the development of the laser gyro an exciting thing to watch.

CHAPTER 5

NUCLEAR GYRO

5.1 Introduction

Nuclear gyros include those known as particle, magnetic induction, nuclear magnetic resonance, and some breeds of solid-state gyros. All are concerned with utilizing the nearly perfect sub-atomic particles of matter in lieu of the gross mechanical parts of convential instruments. Feasibility models have been operated. Results are classified. The principles of operation, however, are not classified and will be here detailed.

Simply put, the principle of operation of the nuclear gyro is as follows. Some nuclei have both an angular momentum and a magnetic moment. In any collection of many such nuclei, the orientation of the individual angular momentum vectors will be random; and the net total angular momentum for the collection will be zero.

However, if a uniform magnetic field is now applied to the collection, an interaction will take place between this field and the individual magnetic moment vectors. Each individual field-moment interaction imparts a torque to that particular nucleus. This torque causes its angular momentum vector to precess about the direction of the applied field. If many nuclei of the collection can be made to respond in this manner, we will have many angular momentum vectors precessing about this one common direction, that of the applied field. Hence, we will have a non-zero net angular momentum in this direction. It is this non-zero net angular momentum and its associated gyroscopic properties with which we are concerned in the nuclear gyro.

These ideas and others will be developed from fundamental concepts in a manner that is intended to appeal to the reader's intuition. It is assumed that the reader is more familiar with gyroscopic principles than he is with electromagnetic and nuclear phenomena. Considerable reference will be made to basic physics (1); to modern (atomic) and nuclear physics (2); and to special treatments in the field of electromagnetics, an exceptionally good one is by Winch (3).

The purpose of this chapter is, of course, to illuminate the basic principles of the nuclear gyro. Accordingly, the content of this chapter is limited; and

only those items which serve that purpose will be here included. On the other hand, however, the authors of this report are of the opinion that such illumination would, in large part, be wasted if it did not enable the reader to further pursue and to comprehend the current open literature. It is for this additional purpose, one which the authors consider inherently necessary in a report of this nature, that the Appendix to Chapter 5 is included. Although the Appendix is considered to be an integral part of the report, the presentation of basic principles will be independent thereof.

In logical sequence, the fundamental concepts will be presented followed by a few comments about electric and magnetic fields. Next to come will be the concept of magnetic moment and its relationship to the angular momentum of a single particle. Having this relationship, we will then be in a position to examine the resulting precession of the single particle's angular momentum vector in a uniform magnetic field. If more than one particle is present, however, complications set in; and a few sections are concerned with these problems. The concluding sections are devoted to applications as manifested by currently operating nuclear gyros.

5.2 Fundamental Concepts

These fundamental concepts underlie the story of the nuclear gyro. An electric field is said to exist if a

non-moving charged particle feels or experiences a force. In contrast, a magnetic field is said to exist if a moving charged particle feels or experiences a force over and above that which a fixed charge would feel. Inasmuch as electrical current is defined as the time rate of flow of charge (1 ampere = 1 coulomb/sec), a charged particle in motion can be considered as a current although no "normal" conduction path exists. Specifically, the orbital motion of the charged electron about its nucleus constitutes a current. (It is remembered that current flow is defined in terms of moving positive charges; hence, the "current" of the negatively charged electron in orbit is opposite to its motion.) Similar to orbital current is the concept of a charged sphere rotating about any diameter (spinning). The charge may be distributed either uniformly or noniniformly and with spin constitutes current. (The special case where the charge is concentrated at a point on the axis of spin is not considered.)

Associated with any mass in rotational motion is, of course, the property called angular momentum. The orbiting electron and the spinning sphere both possess angular momentum. As we shall see, it is the current that gives rise to the magnetic moment; and as already stated, the magnetic moment interacts with an external magnetic field yielding a torque which precesses the

angular momentum vector. The process of setting an angular momentum vector into precession about a known direction is called alignment.

Additional fundamental concepts are these. A magnetic field exists about a current carrying conductor. Faraday's Law states that given a conduction path, an emf (voltage) will be induced in that path that is proportional to the time-rate-of-change of the externally provided magnetic flux linking that path. Lenz's Law states that the current resulting from this induced emf will be in such a direction that its own magnetic field will oppose the change in the externally produced field.

5.3 Electric Field

In regard to an electric field, Coulomb's (experimental) Law gives the force that a unit positive test charge, q', would feel in the vicinity of an arbitrary charge, q:

$$\bar{F}_e = K\frac{qq'}{r^3}\bar{r} \qquad (5.1)$$

where the positive constant of proportionality K is determined by the system of units chosen, and $\bar{r}$ is directed from the arbitrary charge q to the unit positive test charge q'. The electric field intensity $\bar{E}$ is defined as the force per unit positive charge.

$$\bar{E} = \frac{\bar{F}_e}{q'} = K\frac{q}{r^3}\bar{r} \qquad (5.2)$$

If the charged particles have mass, there is, of course, the gravitational mass attraction between them. In particular, the electron of the hydrogen atom is bound by both laws, that of Newton as well as that of Coulomb. However, the Coulomb attraction is approximately 10^{39} times that of Newtonian attraction. Hence, the effects of gravitational attraction are neglected entirely in this discussion.

5.4 Magnetic Field

In regard to a magnetic field, the force that a moving charge feels is given by this vector expression.

$$\bar{F}_m = q\bar{v} \times \bar{B} \qquad (5.3)$$

where $\bar{B}$ is the magnetic flux density and $\bar{v}$ is the velocity of the charge q. Note that the dimension of the product $q\bar{v}$, (coulombs)(meters/second), is the same as the product $i\bar{l}$, (coulombs/second)(meters). These expressions are in fact identical. Hence,

$$\bar{F}_m = i\bar{l} \times \bar{B} \qquad (5.4)$$

where $\bar{l}$ is the vector length of the current path.

Unless otherwise stated, all references to magnetic fields in this report mean externally supplied fields. Enternal fields are assumed to be uniform in the region of interest and of sufficient strength so as to remain essentially undisturbed by the actions to be described. Such fields are available from Helmholtz

coils which are discussed in the appendix.

5.5 Magnetic Moment

Consider a rectangular current-carrying loop of wire in a magnetic field as in Figure 5-1. The normal to the plane of the loop makes an angle ϕ with the direction of the applied field. In accordance with Equation (5.4), $\bar{f}_1$ and $\bar{f}_2$ are computed

$$|\bar{f}_2| = |\bar{f}_1| = iL_1B$$

and shown in the figure.

As can be seen, these forces give rise to a torque $\bar{M}$ directed out of the paper. The magnitude of this torque is given as

$$|\bar{M}| = 2f_1 \frac{L_2}{2} \sin \phi = iL_1L_2B\sin \phi$$

where the product L_1L_2 represents the area of the loop. Hence,

$$|\bar{M}| = iAB\sin \phi$$

If we now define $\bar{A}$ as the area vector normal to the loop in the sense of the right-hand current flow, we can write a vector expression for the torque.

$$\bar{M} = i\bar{A} \times \bar{B} \qquad (5.5)$$

The quantity $i\bar{A}$ is defined as the magnetic moment of the current loop and is symbolized as $\bar{m}$.

$$\bar{m} = i\bar{A} \qquad (5.6)$$

The name magnetic moment arises from the fact that

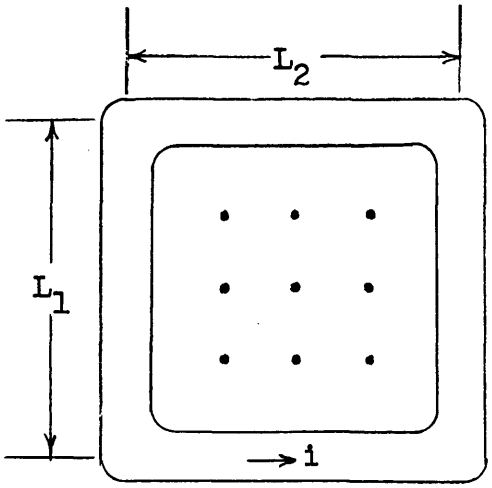

(a)

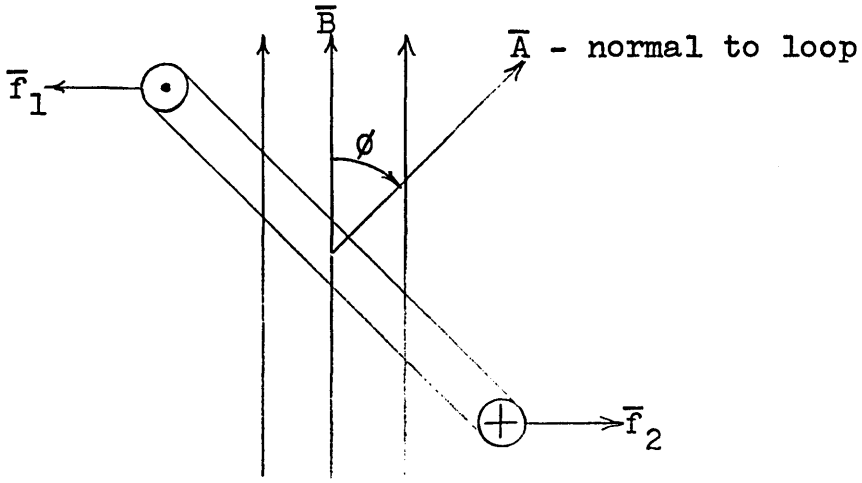

(b)

FIGURE 5-1

CURRENT LOOP IN MAGNETIC FIELD

its magnitude is numerically equal to the moment of force (torque) of magnetic origin that a current loop feels when the plane of the loop is parallel to the direction of a magnetic field of unit flux density.

Although derived specifically for a rectangular current loop, Equation (5.6) is valid for any planar current loop, regular or irregular.

By substituting Equation (5.6) into Equation (5.5), the torque on a current loop can now be expressed

$$\overline{M} = \overline{m} \times \overline{B} \qquad (5.7)$$

Note that the magnetic field gives rise to a torque which tends to align the magnetic moment vector with the direction of the applied field.

5.6 Gyromagnetic Ratio

In order to develop the concept of gyromagnetic ratio, let us consider the hydrogen atom. The hydrogen atom is chosen because of its simplicity. The electron in orbit constitutes a current loop and hence has a magnetic moment $\overline{m}$. The associated angular momentum of the electron in orbit is $\overline{h}$. This angular momentum vector, is of course, normal to the orbital plane in accordance with a right-hand rule and the motion of the electron. The magnetic moment vector is also normal to the orbital plane but opposite in direction from the angular momentum since the current flow is opposite to the electron's

motion. Let us look for a relationship between the angular momentum and the magnetic moment.

The current i is by definition the flow rate of positive charge or charge per unit time. If we assume the orbit to be circular with constant angular velocity ω, the time for one revolution is $2\pi/\omega$. Hence

$$i = -\frac{q}{t} = -\frac{q\omega}{2\pi}$$

where the minus sign signifies that q, when substituted, will be negative; and

$$\bar{m} = -\frac{q\omega}{2\pi}\bar{A}$$

The orbital angular momentum, on the other hand, is

$$\bar{h} = mr^2\bar{\omega}$$

where m without the vector sign refers to mass and r, of course, is the radius.

By noting that the area of the loop is πr^2, we can now write

$$\bar{m} = -\left(-\frac{q\omega}{2\pi}\right)\pi r^2\frac{\bar{h}}{|h|}$$

$$\bar{m} = \frac{q}{2m}\bar{h} \qquad (5.8)$$

where the extra minus sign is introduced to account for the fact that the two vectors have opposite sense. When the electron's negative charge is substituted, opposite

sense prevails.

The scalar multiplicative constant which relates the gyroscopic angular momentum to the magnetic moment of a charged particle in rotational motion, as in Equation (5.8) for example, is logically called the gyromagnetic ratio and is symbolized by γ. The general mathematical statement is as follows.

$$\bar{m} = \gamma \bar{h} \tag{5.9}$$

Note that the gyromagnetic ratio contains the charge to mass ratio of the particle. Hence, the gyromagnetic ratio has the same sign as that of the charge.

$$\begin{aligned} \gamma < 0 \quad & \text{for } + q \\ \gamma > 0 \quad & \text{for } - q \end{aligned} \tag{5.10}$$

At this point, one might question the concern with the magnetic moment vector inasmuch as it is simply a scalar multiple of the angular momentum vector. The answer lies in the theory of quantum physics and will be noted in the appendix. Suffice it here to say that it is the magnetic moment vector that gives rise to the torque of Equation (5.7), and it is the gyromagnetic ratio as it appears in Equation (5.9) that gives us a "handle" on the angular momentum.

5.7 Nuclear Precession

The hydrogen atom used to develop the concept of gyromagnetic ratio was for illustrative purposes only.

Furthermore, it involved the orbital properties of a particle. It is known from modern physics (and included in the appendix) that the electron, in addition to its orbital motion, also spins about its own axis. Likewise, there are "spins" within the nucleus. A spinning proton can be thought of as a spinning charged sphere with associated angular momentum and magnetic moment.

In a given nucleus consisting of several protons and neutrons, the overall spin properties may or may not exist depending on the various orientations within the nucleus. It is known that nuclei of even atomic mass number (sum of number of protons and neutrons) have zero net spin, whereas "odd-numbered" isotopes have non-zero net spin (2). Hence, if spinning nuclei are to constitute the heart of a nuclear gyro, they must be of odd atomic mass number. Furthermore, for a given odd-numbered isotope, the spin may be either plus or minus. More is said on this point in the appendix.

We here assume that the nucleus is of odd atomic mass number. Its angular momentum and magnetic moment are related by its gyromagnetic ratio as in Equation (5.9). Notice here that the nuclear gyromagnetic ratio is a function of both the element (charge) and the isotope (mass). For a particular isotope, it is constant.

There are four equations with which we will be concerned in establishing the precession of the angular

momentum vector of a spinning particle or nucleus. Two of these are Equations (5.7) and (5.9), here repeated.

$$\bar{M} = \bar{m} \times \bar{B} \tag{5.11}$$

$$\bar{m} = \gamma \bar{h} \tag{5.12}$$

The third equation is Newton's third law for rotational motion which relates applied torque to the inertial time derivative of angular momentum.

$$\bar{M} = \left(\frac{d\bar{h}}{dt} \right)_i \tag{5.13}$$

The fourth equation is the vector equation of Coriollis which relates a vector's time derivative in one reference frame to that in another reference frame in terms of the angular velocity of the second frame relative to the first. In particular, we are concerned with the inertial time derivative.

$$\left(\frac{d\bar{C}}{dt} \right)_i = \left(\frac{d\bar{C}}{dt} \right)_{rel} + \bar{\omega}_i \times \bar{C} \tag{5.14}$$

where $\bar{C}$ is any vector, and $\bar{\omega}_i$ is the angular velocity with respect to inertial space of the relative frame of reference. It is assumed that the reader is familiar with these last two equations.

Beginning with Equation (5.13), let us replace the torque on the left hand side by that of Equation (5.11).

$$\bar{m} \times \bar{B} = \left(\frac{d\bar{h}}{dt} \right)_i$$

Solving Equation (5.12) for $\bar{h}$ and substituting yields

$$\bar{m} \times \bar{B} = \frac{1}{\gamma} \left(\frac{d\bar{m}}{dt}\right)_i$$

or

$$\left(\frac{d\bar{m}}{dt}\right)_i = - \gamma \bar{B} \times \bar{m} \qquad (5.15)$$

Let us form the scalar product of both sides of this equation with $\bar{m}$. Notice that the right hand side will be zero since the product $\bar{B} \times \bar{m}$ is normal to $\bar{m}$. Hence,

$$\bar{m} \cdot \left(\frac{d\bar{m}}{dt}\right)_i = 0 \qquad (5.16)$$

By noting the following,

$$\frac{d}{dt}|\bar{m}|^2 = \frac{d}{dt}(\bar{m} \cdot \bar{m}) = 2\bar{m} \cdot \frac{d\bar{m}}{dt}$$

we see that Equation (5.16) tells us that the <u>magnitude</u> of the magnetic moment vector is constant. Hence, its only change can be in <u>direction</u>.

If we now establish a non-inertial frame of reference and attach it to the magnetic moment vector, the time derivative of the vector in this frame will be zero. Hence, Equation (5.15) is seen to be the equation of Coriollis. The motion of the second frame of reference is that of the magnetic moment vector. Hence, the magnetic moment vector precesses about the direction of the applied field with an angular velocity $\bar{\omega}_o$.

$$\bar{\omega}_o = -\gamma \bar{B} \qquad (5.17)$$

Equation (5.17) is the "key" equation for nuclear gyros.

It permits the alignment of the otherwise randomly oriented angular momentum (a scalar multiple of the magnetic moment) to a known direction, that of the applied field. This precession is called Larmor precession.

Recall the earlier assumption that the nucleus did in fact have a magnetic moment. That assumption will be honored throughout this chapter. If the magnetic moment were zero, the nucleus would experience no torque as shown by Equation (5.11). With no torque, the angular momentum would not be aligned by the magnetic field. Hence, Equation (5.17) is not applicable if the magnetic moment is zero.

There is one other situation that warrants comment, and that is the special case when the magnetic moment vector is aligned with the applied field. Notice that the vector cross-product of Equation (5.15) is then zero. That equation does not apply in this special case, and the reason lies in electromagnetic theory. Inasmuch as thermal agitation would not allow the nucleus to remain in a particular orientation for any finite length of time, we will not concern ourselves any further with this special case. Once the magnetic moment is not aligned with the applied field, its response is as given by Equations (5.15) and (5.17).

5.8 Many Nuclei

The preceding discussion has painted a somewhat

"rosy" picture in that it represents the ideal response to an external magnetic field of but one nucleus. We are now in a position to consider the effect of many nuclei. Two effects are of paramont importance. What is the net alignment of the many nuclei and how long does this alignment last?

5.9 Net Alignment

Of the many nuclei present in any macroscopic sample, only a very small fraction of them respond to the external magnetic field (4). Concerning any one of the few that do respond, its net spin may be either plus or minus as pointed out in Section 5.7. With several or more responding, then, some will be precessing in one direction while the rest will be precessing in the opposite direction. Hence, the overall net magnetic moment may be near zero. It is this albeit small net magnetic moment vector that can be aligned. Its response is as given by Equation (5.17) and here repeated.

$$\overline{\omega}_o = -\gamma\overline{B} \qquad (5.17)$$

Note in particular that this "Larmor" frequency is directly proportional to the field strength and inversely proportional to the nuclear mass.

5.10 Characteristic and Relaxation Times

The precessional angular velocity of Equation (5.17) is about the direction of $\overline{B}$. For a particular nucleus,

the magnetic moment vector can be resolved into two components, one perpendicular to $\bar{B}$ that rotates and one parallel to $\bar{B}$ that is constant. If we think of many nuclei in this fashion, it is apparent that the phase relationships of the perpendicular components are random and the net perpendicular component can be said to die out with a characteristic time T_2. The parallel components, on the other hand, assume a Boltzmann distribution (5) in combination and approach the final magnitude with a characteristic time T_1. Occasionally, these times are referred to as relaxation times and are presented here in this fashion in order to contrast with other so-called relaxation times. We will make further mention of T_1 and T_2 later.

Leaving this concept for the moment, let us think of the precessing nuclei as being aligned. Since most of the nuclei are not aligned, one naturally expects interaction between those that are and those that are not. The tendency is for those that are to lose their orientation. Relaxation time refers to the time it takes for a spinning nucleus to lose its orientation. A breakdown of this relaxation time into two causative factors is as follows: spin-spin relaxation time, T_{ss}, which is the time for loss of orientation due to interaction of the nuclear spins amongst themselves; and spin-lattice relaxation time, T_{sl}, which is the time for loss of

orientation due to the changing magnetic field within the lattice. Ordinarily, $T_{ss} \ll T_{sl}$ for solids and $T_{ss} \approx T_{sl}$ for liquids and gases. These times vary from microseconds to hours depending on the material (6,7). In at least one scheme, it is the ratio T_{ss}/T_{sl} that determines the signal to noise ratio (7).

At this point, we have only a small fraction of the available nuclei aligned and the alignment does not persist. Before we can begin to think of readout schemes, some means must be found to align more nuclei, to extend the alignment time, or to do both.

5.11 Nuclear Magnetic Resonance

Nuclear magnetic resonance is a technique to extend the alignment time and is defined by Leighton (2) as that phenomena whereby "nuclei situated in a homogeneous magnetic field are caused to jump from one quantized orientation to another by the application of a weak oscillating field whose frequency is equal to the Larmor precessional frequency of the nucleus in the homogeneous field". In other words, an AC field is synchronized in frequency with $\bar{\omega}_o$ and is a source of "energy bursts" supplied each cycle to the otherwise decaying precession. For this purpose the direction of the AC field is the same as that of the DC field. The precession can be sustained in this manner provided that two conditions exist: the relaxation times (T_{ss} and T_{sl}) and the characteristic times (T_1 and

T_2) must all be long in comparison to the period of the AC field. T_{ss} and T_{s1} must be such in order to prevent alignment decay between energy bursts; T_1 and T_2, in order that the precession not follow the AC field variations. The latter condition is generally met (5).

From Equation (5.17), the period of the precession is

$$T_{\omega_o} = \frac{2\pi}{\gamma B_{dc}} \tag{5.18}$$

Hence,

$$\frac{2\pi}{\gamma B_{dc}} < T_{ss} \leq T_{s1}$$

or

$$B_{dc} > \frac{2\pi}{\gamma T_{ss}} \tag{5.19}$$

This is an important relationship yielding the minimum magnetic flux density necessary to sustain alignment. The AC field flux density must be somewhat less than this, usually 1/2 or less of B_{dc}, for maximum resonance phenomena.

If the relaxation times are sufficiently long, bursts of energy can be supplied less frequently than every cycle. However, the "bursts" must always be synchronized. Hence, some nuclear gyros might use some subharmonic frequency of $\overline{\omega}_o$ for the AC field.

Note also that in accordance with Equation (5.17), the DC magnetic field must be known accurately in order to know the frequency of precession which is also the fundamental frequency of the AC field.

$$\omega_{B_{ac}} = \omega_o = \gamma B_{dc} \qquad (5.20)$$

If magnetic flux density variations are expected, such as from foreign external fields or power supply variations, then means must be provided to change the frequency of the AC field accordingly. An effective way to circumvent this necessity by other than cryogenic shielding will be illuminated shortly.

If another coil surronds our sample of material, the precessing magnetic moment vectors constitute a changing flux linkage. Hence, a signal will be induced therein. This phenomena is known as nuclear magnetic induction. However, unless some means can be found to get the random phases of the precessing nuclei "in step" with one another, Larmor precession can only be detected in this manner as noise (8). Noise signal strength can be used to detect nuclear magnetic resonance, however.

5.12 Optical and RF Pumping

Optical pumping is defined by Bitter (8) as the "selective population of any (quantized) state by optical means". As an example, take the case of the laser covered in Chapter 4. The atoms could have been excited

from the n = 1 to the n = 2 level by optical means. The application to nuclear gyros is somewhat different, however,

An interesting application of optical pumping has been employed by General Precision, Inc., (GPL) in their nuclear gyro which serves to align many more nuclei than would otherwise be aligned (9). As pointed out in Section 5.9, some of the nuclei will be precessing in one direction while the remainder, in the opposite direction. Visualize that situation as though you were looking in the direction of the magnetic flux density $\overline{B}$. You would see some vectors going clockwise, others, counterclockwise.

Now let us propagate circularly polarized light (10) in the direction we are looking. Let the $\overline{E}$ vector of the light electromagnetic wave be rotating, say, clockwise. This clockwise rotating light has no effect on the clockwise-spinning nuclei but is absorbed by the counterclockwise-spinning nuclei which "pumps" or transfers them to the opposite spin state (8). Hence, the precession of these nuclei is also reversed so that they, too, are precessing clockwise. This technique has enabled GPL to increase the number of aligned nuclei from one out of every million to nearly one out of every five (4). Further improvements here may be expected in view of the fact that up to 90 % "alignment" has been achieved in

other applications (8).

Radio Frequency (RF) pumping is employed by ARMA (7) to increase by a factor of three (in some materials) the number of aligned protons. According to the report, the RF field aligns the electrons which in turn align additional protons. The process is called cross-relaxation. RF fields can also be used to lend some degree of coherence (see Chapter 4) to the phase relationship of the precessing nuclei (8).

5.13 Applications and Readout

Although no nuclear gyros had been reported operating at the time of his paper, Culver (6) offered a number of proposals that nevertheless make interesting reading today. His proposals involved the use of cryogenic shielding (see Chapter 3) which is not necessary in some nuclear gyros now operating. He points out, however, that any electric or magnetic field that would be large enough to be used in a readout scheme would inherently disrupt the alignment we were trying to observe. Thus other means must be found; indeed, they have been found.

The current open literature on nuclear gyros pertain, for the most part, to the work of two companies: Republic Aviation (5, 11) and General Precision, Inc., (GPL) (4, 9, 12, 13). Others include American Bosch Arma (7), General Electric, and Sperry. A brief descrip-

tion of the products of the first two companies follows. Unless otherwise noted, the source of information is the respective references just indicated. A complete description of those references will not be made here.

The Republic device is a "two-degree-of-freedom" rate sensor where the two input axes together with the direction of the DC (and AC) field form a mutually orthogonal triad. Their theory begins with the equation of Coriollis [Equation (5.14)] and Equation (5.15).

$$\left(\frac{d\bar{m}}{dt}\right)_i = \left(\frac{d\bar{m}}{dt}\right)_{rel} + \bar{\omega}_i \times \bar{m} = \gamma \bar{m} \times \bar{B}_{dc} \qquad (5.21)$$

where i refers to inertial space. In Section 5.7 we showed $(d\bar{m}/dt)_{rel}$ to be zero; that relative frame was attached to the vector. The relative frame here is that of the observer. Hence, from Equation (5.21),

$$\left(\frac{d\bar{m}}{dt}\right)_{rel} = \gamma \bar{m} \times \left(\bar{B}_{dc} + \frac{\bar{\omega}_i}{\gamma}\right) \qquad (5.22)$$

They observe at this point that inertial rotations can be simulated by an additional magnetic field of flux density $\bar{B}_i$.

$$\bar{B}_i = \frac{\bar{\omega}_i}{\gamma} \qquad (5.23)$$

Also observed at this point: if an inertial rotation not in alignment with $\bar{B}_{dc}$ is applied for a length of time long in comparison to the characteristic times T_1 and T_2,

the alignment of the magnetic moment vectors will change from that of $\overline{B}_{dc}$ to that of the vector sum

$$\overline{B}_{sum} = \overline{B}_{dc} + \overline{B}_i \qquad (5.24)$$

It is this "leaning" of the precessing magnetic moment vectors in the direction of the inertial rotation that permits a signal to be induced in a coil whose axis represents an input axis of the device. Hence, we have a nuclear magnetic induction gyro.

This arrangement appears to have inherent limitations. Inertial rotations that last for times short compared to T_1 and T_2 may go undetected. These times were on the order of 300 microseconds in 1962 using water doped with a paramagnetic salt. (Magnetic classification of materials is covered in the appendix.) Since $\overline{\omega}_i$ or equivalently $\overline{B}_i$ is at right angles to $\overline{B}_{dc}$, its magnitude must be limited in order to preserve linearity and channel integrity.

$$\left|\overline{\omega}_i\right| < \gamma \left|\overline{B}_{dc}\right|$$

When inertial rotations (actual or simulated) are at right angles to $\overline{B}_{dc}$ as is the case, the precession of the magnetic moment vectors is a highly perturbed elliptic path about $\overline{B}_{sum}$. The precession induces a signal in coils which surround the sample and harmonic analysis is necessary for readout. They use the second

harmonic of ω_o and find it to be maximum when $B_{ac} = 2B_{dc}$. B_{dc} was 6.11 Gauss; ω_o, 26 kc. Signal voltage after two stages of amplification was in the microvolt region. Good magnetic shielding was necessary.

The GPL device is a single-degree-of-freedom integrating gyro whose sensitive axis corresponds to the direction of $\bar{B}_{dc}$. The core material is a vapor consisting of two isotopes of mercury, 199 and 201. Optical pumping as previously described is used to align more nuclei and magnetic resonance techniques sustain alignment.

Simpson et al. (9) of GPL begin their theory with reference to the work of Packard and Weaver (14) in 1951. The beginning equation is

$$\omega_1 = - \gamma B_{dc} + \omega_i \qquad (5.26)$$

where ω_1 = apparent or observed precessional angular velocity, and ω_i = inertial angular velocity of observer about the direction of $\bar{B}_{dc}$. The two isotopes used by GPL have different atomic mass numbers. Hence, for them

$$\begin{aligned} \omega_1 &= - \gamma_1 B_{dc} + \omega_i \\ \omega_2 &= - \gamma_2 B_{dc} + \omega_i \end{aligned} \qquad (5.27)$$

Assume for the moment that some method exists by which ω_1 and ω_2 may be measured. γ_1 and γ_2 are known. B_{dc} and ω_i may be treated as unknowns. With these equations we can eliminate B_{dc} and solve for ω_i.

$$\omega_1 = \frac{\gamma_1\omega_2 - \gamma_2\omega_1}{\gamma_1 - \gamma_2} \qquad (5.28)$$

Hence, the magnitude of B_{dc} need not be known to any great accuracy but it must be reasonably stable.

Actual readout is somewhat different. A second light beam is passed through the sample at right angles to the direction of $\overline{B}_{dc}$. This beam is amplitude modulated by the precessing nuclei at the apparent precessional frequency and detected (on the other side of the sample) by a photo-multiplier tube. The tube's output is amplified and contains the two apparent angular velocities ω_1 and ω_2 or, alternatively, f_1 and f_2. In the reported configuration, the amplifier output is also the source of synchronization for the AC field to sustain precession. This configuration is called a spin generator.

Although this design does not encounter the same problem at high angular velocity inputs as does the previous design, another appears to us. Inasmuch as the nuclei are precessing with respect to inertial space, the energy "bursts" supplied should be likewise synchronized. This is not the case in the reported design where the energy bursts are derived from the apparent precession.

In a field of density 1.3 Gauss, f_1 = 1000 cps and f_2 = 367 cps. Using these numbers and rearranging Equations (5.27) yields

$$f_1 = -1000\frac{\dot{B}}{1.3} + \frac{\omega}{2\pi}$$

$$f_2 = -\ 367\frac{\dot{B}}{1.3} + \frac{\omega}{2\pi}$$

If the field were to change by, say, 1 %, δf_1=10 cps while δf_2=3.67 cps. Inertial inputs, on the other hand, cause $\delta f_1=\delta f_2=\omega/2\pi$. This fact permits discrimination between a change in the magnetic field and an inertial input. It also permits automatic regulation of B_{dc}. Hence, only moderate magnetic shielding is necessary.

With small inertial inputs, recourse is necessary to phase comparison (for readout) of the two signals, one of which is nearly the third harmonic of the other. This problem is one of instrumentation and does not inherently limit detection capability. Run-up time is about five seconds (15). Further improvements have already been made to the basic design, some of which are reported in the open literature; they will not be reported here.

5.14 Conclusion

The development of the nuclear gyro constitutes a radical departure from conventional thoughts. Such is usually the case when conventional performance begins to level off. The estimated future detection capability of nuclear gyros is 0.0001 degrees/hour (15) - that's one revolution in 410 years. Perhaps further study into the

motions of our universe will soon be feasible.

In addition to fantastic sensitivity, the nuclear gyro offers indefinite life, zero drift due to friction, almost instantaneous run-up, only infinitesimal inertia reaction on a space craft that might be carrying it, low cost, and competitive size, weight, and power requirements. Its development should be watched.

APPENDIX

TO

CHAPTER 5

A5.1 Introduction

This appendix is intended to complement the basic principles of nuclear gyros as presented in Chapter 5. If one were to read two articles on nuclear gyro developments, he would probably find two systems of notation. Perhaps this report constitutes a third. Nevertheless, this appendix is included to make such reading more rapid. References here are the same as those of Chapter 5.

A5.2 Helmholtz Coils (3)

Reference is frequently found to Helmholtz coils. These are nothing more than a means of obtaining a uniform magnetic field, uniform in both magnitude and direction.

Two circular coils of equal radius are constructed. They are arranged parallel to each other on a common axis. The distance between them is made equal to the coils' radius. This arrangement is called a Helmholtz

coil pair, named for its inventor.

If equal electric currents are made to flow in the same direction in both coils, a uniform magnetic field will exist in the center region. The direction of this field is that of the common axis, and the flux density is as follows.

$$B = 9 \times 10^{-7} \frac{NI}{r} \qquad \text{(RMKS)} \qquad \text{(A5.1)}$$

where B is in webers/meter^2 and (NI/r) is the ampere-turns per meter of one of the coils.

For the cgs system of units,

$$B = 90 \frac{NI}{r} \qquad \text{(cgs)} \qquad \text{(A5.2)}$$

where B is in Gauss and (NI/r) is the ampere-turns per centimeter of one of the coils.

A5.3 Electron and Nuclear Spin Properties

In Section 5.6, we considered the orbital properties of the hydrogen atom's electron. We then proceeded directly to nuclear spins. The purpose of this section is to fill that void.

In the early 1920's, spectroscopists were observing phenomena that they could not explain with the then-existing integral quantum number theories of atomic physics. Successful explanation was made by Uhlenbeck and Goudsmit when they assumed that the electron itself possessed both angular momentum and magnetic moment apart from its or-

bital properties. This theory is now firmly established in modern physics (2) and these inherent particle characteristics are referred to as spin properties.

The relationship between spin magnetic moment and spin angular momentum is also a linear one and was measured by Barnett (16). It is given as

$$\bar{m}_s = - \frac{q}{m} \bar{h}_s \qquad (A5.3)$$

Hence,

$$\gamma_s = - \frac{q}{m} = 2\gamma_{or} \qquad (A5.4)$$

Since the spin gyromagnetic ratio is twice the orbital value, it is conceivable that under certain circumstances spin properties might dominate over orbital properties. Barnett (16) has shown that this fact is indeed responsible for the classic magnetic behavior of iron.

The inclusion of electron spin in the theory of aromic physics satisfactorily explained the "fine structure" of spectroscopy. Yet discrepancies still existed in that they were unable to explain what is now known as the "hyperfine structure". Inclusion was made here of spins within the nucleus.

Nuclear spin angular momentum for hydrogen has the same magnitude as that of the electron. With reference to Equation (A5.3), one would expect that the nuclear

magnetic moment would be 1/1836 times the electron value since the mass of the proton is 1836 times that of the electron. Such is not the case, however. The nuclear magnetic moment turns out to have a magnitude 2.8/1836 times that of the electron (3).

Even though the nucleus may have spin angular momentum of the order of that of spinning electrons, its magnetic moment is generally small in comparison thereto. Herein lies the justification for dealing with the magnetic moment vector, the quantity that gives rise to the torque.

Thus we have three vectors (orbital, electron spin, and nuclear spin) for both angular momentum and magnetic moment. Hence, for any particular atom it is the vector sum that determines the net quantities. For an atom to be aligned via an external magnetic field as previously described, its net magnetic moment vector must be non-zero.

It will be noted that the three relationships between angular momentum and magnetic moment have been separately stated. Any attempt to couple the three realms would soon be involved in the mathematics of quantum physics. Such is not the purpose of this report. However, some considerstion of spin-orbit interaction is both necessary and inevitable in any study of nuclear gyros.

A5.4 Literature Notation

The definition of magnetic moment presented by Equation (5.6) is in accordance with the Sommerfeld proposal and is used exclusively throughout this report. one might encounter, however, another definition in the literature. This other definition is

$$\bar{m} = \mu_o i\bar{A}$$

where μ_o is the permeability of free space (3). This latter definition is in accordance with the Kennelly proposal but will be found only rarely, if at all, in the literature on nuclear gyros.

The Bohr theory says that the energy of an atom can exist only in discrete quantities. It was later found that within each discrete energy level, a further breakdown was necessary into discrete quantities of angular momentum. It was at this point, historically, to which spectoscopists had arrived in the early 1920's. The inclusion of electron spin to explain the fine structure resulted in a further division of the angular momentum into discrete quantities. Then of course came the nuclear spin for the hyperfine structure.

In the theory of quantum physics, reference is made not only to the magnitude of certain quantities but also to the so-called Z component of vector quantities where the Z axis is any particular direction in space.

The unit of angular momentum is Planck's constant (6.625×10^{-34} $m^2 kg/sec$) and is symbolized by the scalar h. Much more frequently encountered, however, is $h/2\pi$. This latter quantity is designated $\hbar$. Note the distinction between this notation and that of the angular momentum vector, $\bar{h}$. Quantites of angular momentum are specified in terms of some number, the angular momentum quantum number, times $\hbar$.

$$\begin{aligned} h &= \text{Planck's constant} \\ \hbar &= h/2\pi \\ \bar{h} &= \text{angular momentum vector} \end{aligned} \qquad \text{(A5.5)}$$

The Z axis component of <u>orbital</u> angular momentum can have integral quantum numbers. In contrast, the Z axis component of <u>spin</u> angular momentum can have only two half-integral quantum numbers, $\pm$ 1/2.

$$\left|\bar{h}_s\right|_z = \pm \frac{\hbar}{2} \qquad \text{(A5.6)}$$

Using this in Equation (A5.3), the Z axis component of the spin magnetic moment vector is given as

$$\left|\bar{m}_s\right|_z = \pm \frac{q\hbar}{2m} \qquad \text{(A5.7)}$$

This quantity is called the <u>Bohr magneton</u> and represents a unit of spin magnetic moment. It is encountered frequently and with varying designations. Sometimes it is μ or μ_o; mostly it's μ_b.

$$\mu_b = \frac{q\hbar}{2m} \qquad (A5.8)$$

The nuclear magneton was defined in like manner and is given as

$$\mu_n = \frac{q\hbar}{2m_p} \qquad (A5.9)$$

where m_p is the proton mass. As mentioned earlier, however, the proton magnetic moment is 2.8 times this value.

$$\mu_p = 2.8\ \mu_n \qquad (A5.10)$$

Another frequently encountered item is the vector $\bar{I}$ which is defined by this relationship:

$$\bar{h}_n = h\ \bar{I} \qquad (A5.11)$$

Hence, $\bar{I}$ is seen to be a"vectorized" quantum number associated with nuclear spin angular momentum.

Combining these last two equations yields an expression of this sort,

$$\bar{\mu} = K\mu_n\bar{I} \qquad (A5.12)$$

where K = 1 and $\bar{I}$ = 2.8 for the single proton. An equation of this type is frequently the beginning point of nuclear gyro articles. For other than a single proton, K might vary from -4 to +4 in the expression for the nuclear magnetic moment (6).

A5.5 Larmor Precession

Larmor precession is a manifestation of spin-orbit

interaction and refers to spin precessions. This interaction, in turn, falls back on electromagnetic theory. No external magnetic field is necessary for this precession. Larmor precession is the non-relativistic precession of the spin magnetic moment vector in the internally generated magnetic field B'.

$$\bar{\omega}_L = - \gamma_s \bar{B}' = \frac{q}{m} \bar{B}' \qquad \text{(A5.13)}$$

The internal field for hydrogen is given by Leighton (2) as

$$\bar{B}' = \frac{K}{r^3 c^2} \frac{q}{m} \bar{h}_{or} \qquad \text{(A5.14)}$$

where K is the same constant as in Equation (5.1); r and c are the orbital radius and speed of light, respectively. No further reference will be made to this field. In the literature on nuclear gyros, the term "Larmor precession" is generally used to denote the precession of any magnetic moment vector in any magnetic field.

A5.6 Magnetic Classification of Materials

The classic definitions that arise here are covered well in most introductory treatments of electricity and magnetism. In the interest of completeness, they will be stated here but without elaboration.

A diamagnetic material is one whose atoms have a zero net magnetic moment vector; a paramagnetic material is one whose atoms have a non- zero net magnetic moment

vector; and a ferromagnetic material is one that exhibits unusually large paramagnetic behavior.

Winch (3) points out that even in an atom which is paramagnetic by definition, the diamagnetic effect is still present. For our nuclear gyro purposes, then, the paramagnetic effect must dominate.

A5.7 Bar Magnet Analogy

Many (if not most) of the current references on nuclear gyros contain in one form or another some analogy to bar magnets in the discussion of torques. This in undoubtedly due to an assumed lack of familiarity with magnetic moments on the part of the reader. We feel that this analogy will gradually vanish as knowledge is gained. Nevertheless, it exists today and for that reason warrents inclusion here.

The idea is simple. Given a bar magnet and an externally produced magnetic field which is initially not aligned with the length of the bar, the bar receives a torque which tends to align its length with the direction of the external field. This is the principle of the simple compass. Experimental and measureable data yielded the torque equation, Equation (5.7), which is here considered to be the defining equation for the magnetic moment $\bar{m}$ of a bar magnet. Its direction is along the length of the bar from the south-seeking to the north-seeking pole. Occasional reference might be found to the pole strength

of a bar magnet. Pole strength is a scalar quantity and is defined as the ratio of the magnitude of the magnetic moment vector to the distance between the centers of the two "poles" of the bar magnet. This distance is in general somewhat less than the physical length of the bar.

REFERENCES

CHAPTER 2

1. Knoebel, H. W., "The Electric Vacuum Gyro", Control Engineering, February, 1964.

2. Smythe, W. R., Static and Dynamic Electricity, McGraw-Hill Book Co., 1950.

3. Winch, R. P., Electricity and Magnetism, Prentice-Hall Inc., 1957.

4. Nordsieck, A., "Principles of Electric Vacuum Gyroscopes", ARS Guidance and Control Conference, 7-9 August, 1961.

5. Harness, G. T., and Hehre, F. W., Electrical Circuits and Machinery, John Wiley and Sons Inc., 1942.

6. Klass, P. J., "Inertial System Uses Electrostatic Gyros", Aviation Week and Space Technology, September 30, 1963.

CHAPTER 3

1. Shoenberg, D., Superconductivity, Cambridge at the University Press, 1962.

2. Buchhold, T. A., "The Magnetic Forces on Superconductors and Their Application for Magnetic Bearings", Cryogenics, June, 1961, 203-205.

3. LaFond, C. D. "GE's New Cryogenic Gyros Near Testing", Missiles and Rockets, July 24, 1961.

4. Culver, W. H., and Davis, M. H., "An Application of Superconductivity to Inertial Navigation", The Rand Corporation, January 7, 1957.

5. Harding, J. T., and Tuffias, R. H., "Cryogenic Gyros Levitated by Magnetic Repulsion", Space/Aeronautics, September, 1961, 133-141.

CHAPTER 4

1. Landau and Lifshitz, Classical Theory of Fields, Chapter 10, translated from the Russian by Morton Hamermesh, Pergamon Press and Addison Wesley, 1962.

2. Terman, F. E., Electronic and Radio Engineering, McGraw-Hill, N. Y., 1955, 1033.

3. Holahan, J., "Coherent Light as Data Carrier", Space/Aeronautics, April 1962.

4. Leighton, R. B., Principles of Modern Physics, McGraw- Hill, 1959.

5. Brinley, B. R., "The Maser", Microwave Journal, August 1962.

6. Oliver, B. M., "Some Potentialities of Optical Masers", Proceedings of the IRE, February 1962.

7. Javan, Ballik, and Bond, letter in Journal of the Optical Society of America, Vol. 52, 1962, 96.

8. RSK, "Sperry Ring Laser Rotation Rate Sensor, Technical Data", February 5, 1963.

9. White, G. R., "The Laser Gyroscope", Sperry Gyroscope Company, May 1963.

10. White, G. R., personal letter to J. W. Harrill, April 7, 1964.

11. Sperry Advertisement, Aviation Week and Space Technology, Volume 80, No. 15, April 13, 1964, 18.

12. LaVan, J. T., "Unconventional Inertial Sensors", Space/Aeronautics, Vol. 40, No. 7, December, 1963, 73-83.

13. Zito, R. Jr., "Velocity Sensing for Spacecraft Docking", Space/Aeronautics, Vol. 40, No. 7, Dec. 1963.

14. Langford, R. C., "Guidance and Control", Astronautics and Aerospace Engineering, Vol.1, No. 10, November, 1963, 117.

CHAPTER 5

1. Sears, F. W., and Zemansky, M. W., University Physics, Addison-Wesley, Reading, Mass., 1955.

2. Leighton, R. B., Principles of Modern Physics, McGraw-Hill, New York, 1959.

3. Winch, R. P., Electricity and Magnetism, Prentice Hall, N. J., 1955.

4. Klass, P. J., "New Gyro Uses Mercury Isotope Mixture", Aviation Week and Space Technology, Vol. 79, No. 7, Aug. 12, 1963, 88-93.

5. Minneman, M. J., "Drift Minimized in Magnetic Induction Gyro", Space/Aeronautics, Vol. 38, No. 6, Nov. 1962, 79-82.

6. Culver, W. H., "Nuclear Gyros", ARS Paper No. 1948-61; or ARS Journal, Vol. 32, No. 6, Jun 1962, 943-944.

7. Wolff, M. F., "Solid-State Nuclear Gyro Reported Feasible", Electronics, Vol. 35, No. 52, Dec. 28, 1962, 48-51.

8. Bitter, F., "Magnetic Resonance in Radiating or Absorbing Atoms", Applied Optics, Vol.1, No. 1, Jan. 1962, 1-10.

9. Simpson, J. H., Jr., Fraser, J. T., and Greenwood, I. A., Jr., "An Optically Pumped Nuclear Magnetic Resonance Gyroscope", IEEE Transactions on Aerospace, Vol. AS-1, No. 2, Aug. 1963, 1107-1110.

10. Bitter, F., Currents, Fields, and Particles, Part II, Technology Press, 1955.

11. Forman, S. M., and Minneman, M. J., "A Magnetic Induction Gyroscope", IEEE Transactions on Military Electronics, Vol. MIL-7, No. 1, Jan. 1963.

12. (no author listed), "Nuclear Gyro - It Really Works", Electronics, Vol. 36, No. 3, Jan. 18, 1963, 18.

13. "Spinning Nuclei Signal Angular Displacement in Mercury-Isotope Gyro", Engineering News section of Machine Design, Vol. 35, No. 20, Aug. 29, 1963, 10.

14. Packard, M. E. and Weaver, H. E., "Nuclear Relaxation Time for Hydrogen Gas", Physical Review, Vol. 88, 1952, 163

15. LaVan, J. T., "Unconventional Inertial Sensors", Space/Aeronautics, Vol. 40, No. 7, Dec. 1963, 73-83.

16. Barnett, S. J., "Gyromagnetic and Electron-Inertia Effects", Reviews of Modern Physics, Vol. 7, 1935, 129.